Thesis for the degree of licentitate

Geometric Spectral Invariants and Isospectrality

Gustav Mårdby

Department of Mathematical Sciences

Division of Analysis and Probability Theory

Chalmers University of Technology and the University of Gothenburg

Göteborg, Sweden 2025

Geometric Spectral Invariants and Isospectrality

Gustav Mårdby

©Gustav Mårdby, 2025

Department of Mathematical Sciences Division of Analysis and Probability Theory Chalmers University of Technology and the University of Gothenburg SE-412 96 Göteborg Sweden

Typeset with LATEX Printed by Chalmers Reproservice Göteborg, Sweden 2025

Geometric Spectral Invariants and Isospectrality

Gustav Mårdby

Department of Mathematical Sciences

Division of Analysis and Probability Theory

Chalmers University of Technology and the University of Gothenburg

Abstract

This thesis investigates how geometric features of domains are reflected in the spectrum of the Laplacian, a central theme in spectral geometry. In Chapter 1, we introduce the subject and explain classical results and questions, such as Weyl's law, Milnor's 16-dimensional pair of flat tori, and Kac's question "Can one hear the shape of a drum?" In Chapter 2, we study integrable polygonal domains and obtain explicit expressions for associated spectral invariants, including the spectral zeta function and the heat trace. We show that, for this class of polygons, the length of the shortest closed geodesic appears in the remainder of the heat trace expansion. We also analyze the convergence of heat trace coefficients under geometric limits between convex polygons and smooth domains. Chapter 3 presents the first ever example of a 6-dimensional triplet of isospectral but non-isometric flat tori, and we explain how it relates to previously known results. In Chapter 4, we study the short-time heat trace expansion of convex polygons with Neumann boundary conditions and obtain an explicit remainder estimate using locality principles, extending results previously known only in the Dirichlet case. Finally, in Chapter 5, we conclude by summarizing the main contributions of the thesis and outlining directions for future research.

Keywords: Spectral geometry, Laplace operator, eigenvalues, heat trace, isospectrality, integrable polygons, spectral determinant, shortest closed geodesic, flat tori, locality principles

Acknowledgements

I want to express my deepest gratitude to my supervisor, Julie Rowlett, for her encouragement, support, generosity in sharing her ideas and knowledge, and for many insightful discussions. Her enthusiasm and guidance have been truly invaluable, and she has been an outstanding supervisor in every way. I am also very grateful to my co-supervisor, Simon Larson, for his clever ideas and insights, continuous support, and for checking on me regularly. I would like to thank my co-author, Felix Rydell, for the good teamwork and many nice discussions. I would also like to thank Jeffrey Steif for the inspiring conversations and challenging questions that encouraged me to think outside the box. Big thanks to all my coworkers for making my time at the university both enjoyable and memorable, and to all the professors in the department for offering such fascinating and inspiring courses. Finally, I am deeply thankful to my friends and family for their endless love, support, and encouragement throughout this journey.

Gustav Mårdby Göteborg, 2025

Contents

A	bstra	act	i		
A	ckno	wledgements	ii		
Li	st of	publications	v		
1	A c	entury of spectral geometry	1		
	1.1	Main results of Paper 1	6		
2	Spectral invariants of integrable polygons				
	2.1	Spectral zeta function	8		
	2.2	Heat trace expansion	13		
	2.3	Convex polygons and smoothly bounded domains	17		
3	Three's company in six dimensions				
	3.1	Search algorithm	26		
	3.2	Isospectrality	28		
	3.3	Non-isometry	31		
	3.4	Irreducibility	32		
	3.5	Choir numbers	33		
4	Bey	ond three terms: Neumann heat trace of convex			
	pol	ygons	35		
	4.1	Locality principles	36		
	4.1	Locality principles			

iv Contents

	4.2	Heat trace	41				
	4.3	Compact polyhedral surfaces	44				
5	5 Conclusions and future work						
	5.1	Integrable polytopes and convergence of polygons	47				
	5.2	Isospectral flat tori and choir numbers	49				
	5.3	Heat trace expansion for Neumann polygons	51				

List of publications

This thesis consists of an extended summary and the following appended manuscripts.

- Paper 1: Mårdby, G., Rowlett, J. A century of spectral geometry from Weyl to Milnor, Kac and beyond. (2024) Conditionally accepted pending revision to Reviews in Mathematical Physics.
- Paper 2: Mårdby, G., Rowlett, J. Spectral invariants of integrable polygons. (2024) Accepted and published in Journal of Fourier Analysis and Applications.
- Paper 3: Mårdby, G., Rowlett, J., Rydell, F. Three's company in six dimensions: irreducible, isospectral, non-isometric flat tori. (2024) Conditionally accepted pending revision to Proc. AMS.
- Paper 4: Mårdby, G. Short-time asymptotics of the Neumann heat trace on convex polygons via locality principles. (2025) Manuscript.

Author contribution:

- **Paper 1:** I wrote the proof of Weyl's law, explained Milnor's counterexample, and contributed to the writing and calculations of every section.
- **Paper 2:** I proved every theorem, every proposition, every corollary, and every lemma. I also contributed to the writing.
- **Paper 3:** I found the triplet, proved every main theorem, and contributed to the writing and coding.
- Paper 4: I carried out all the research and writing for this paper.

Chapter 1

A century of spectral geometry

Spectral geometry is the study of the interplay between geometric structures and the spectra of differential operators defined on them. A central object in this field is the Laplace operator, which in Euclidean space \mathbb{R}^n is defined by

$$\Delta = -\sum_{i=1}^{n} \frac{\partial^2}{\partial x_i^2}.$$
 (1.1)

When restricted to a bounded domain $\Omega \subset \mathbb{R}^n$, the Laplace operator gives rise to the eigenvalue problem

$$\Delta u = \lambda u \text{ in } \Omega, \tag{1.2}$$

together with some boundary conditions. The two most common boundary conditions are the *Dirichlet boundary conditions* and the *Neumann boundary conditions*. The former requires the functions to vanish at the boundary,

$$u|_{\partial\Omega}=0,$$

and models e.g. a membrane whose boundary is held fixed. The latter requires the outward normal derivative on $\partial\Omega$ to vanish at the boundary,

$$\left. \frac{\partial u}{\partial n} \right|_{\partial \Omega} = 0,$$

and models e.g. an insulated boundary in the heat equation, where no heat flows across the boundary.

Given the boundary conditions, the real numbers λ for which there exists a non-trivial solution to (1.2) are called eigenvalues, and the corresponding solutions u are called eigenfunctions. The collection of all eigenvalues λ is known as the spectrum of Ω . In physical applications, the spectrum describes the resonant frequencies of vibrating membranes, the rate at which heat diffuses through a medium, and the energy levels of quantum systems (Kac, 1966). For unbounded domains or non-compact Riemannian manifolds, the spectrum may, in addition to the eigenvalues, include continuous components known as the essential spectrum. However, for most domains considered in this thesis, including bounded domains with Dirichlet boundary conditions or bounded domains with Lipschitz boundary and Neumann boundary conditions, the spectrum is always discrete and coincides with the set of eigenvalues (Borthwick, 2020, Thm. 6.8). This discreteness allows one to arrange the spectrum as an infinite, increasing sequence of real numbers tending to infinity,

$$0 \le \lambda_1 \le \lambda_2 \le \lambda_3 \le \dots \uparrow \infty$$
,

where each eigenvalue is repeated according to its multiplicity. In the Dirichlet case we always have $\lambda_1 > 0$, whereas in the Neumann case we have $\lambda_1 = 0$ with multiplicity one, provided that Ω is connected (Levitin et al., 2023, Prop. 2.1.21, Remark 2.1.34). In either case, the corresponding eigenfunctions $\{u_k(x)\}_{k\geq 1}$ form an orthogonal basis for $L^2(\Omega)$. Understanding the asymptotic distribution of these eigenvalues is a central theme in spectral geometry. A classical and fundamental result on this is Weyl's law (Weyl, 1912), which relates the growth of eigenvalues to the volume of the underlying domain or manifold. More precisely, Weyl's law states that the counting function

$$N(\lambda) = \#\{k : \lambda_k \le \lambda\}$$

grows asymptotically like

$$N(\lambda) \sim \frac{\omega_n |\Omega|}{(2\pi)^n} \lambda^{n/2}, \ \lambda \uparrow \infty,$$
 (1.3)

where $\omega_n = \frac{\pi^{n/2}}{\Gamma(n/2+1)}$ is the volume of the unit ball in \mathbb{R}^n . One way to prove Weyl's law is to begin with Euclidean boxes, for which one can use separation of variables to obtain the eigenvalues explicitly. For a general bounded domain with Dirichlet boundary conditions, one then approximates the domain from inside and outside with finite unions of small boxes and uses domain monotonicity for the eigenvalues (Borthwick, 2020, Thm. 6.20). See Paper 1 for details.

Another tool for understanding the spectrum is through the heat equation

$$\begin{cases} \left(\frac{\partial}{\partial t} + \Delta\right) u(t, x) = 0 \text{ in } (0, \infty) \times \Omega, \\ \frac{\partial u}{\partial n} = 0 \text{ on } (0, \infty) \times \partial \Omega, \\ u(0, x) = f(x) \text{ in } \Omega. \end{cases}$$
(1.4)

Here, $f \in L^2(\Omega)$ is given. The fundamental solution of the heat equation is called the *heat kernel*. The heat kernel $H_{\Omega}: (0, \infty) \times \Omega \times \Omega \to \mathbb{R}$ satisfies

$$\left(\frac{\partial}{\partial t} + \Delta\right) H_{\Omega}(t, x, y) = 0 \text{ assuming } \Delta \text{ acts in either } x \text{ or } y,$$

$$H_{\Omega}(t, x, y) = H_{\Omega}(t, y, x),$$

$$\lim_{t \downarrow 0} H_{\Omega}(t, x, y) = \delta(x - y) \text{ in the sense of distributions,}$$

and the heat equation (1.4) has the solution

$$u(t,x) = \int_{\Omega} H_{\Omega}(t,x,y) f(y) dy.$$

Moreover, if $\{u_k(x)\}_{k\geq 1}$ is an orthonormal basis for $L^2(\Omega)$ consisting of eigenfunctions with corresponding eigenvalues λ_k , then we have (see (Levitin et al., 2023, Thm. 6.1.2))

$$H_{\Omega}(t, x, y) = \sum_{k=1}^{\infty} e^{-\lambda_k t} u_k(x) u_k(y), \ x, y \in \Omega, \ t > 0.$$

The heat trace of Ω is defined as

$$h_{\Omega}(t) := \int_{\Omega} H_{\Omega}(t, x, x) dx = \sum_{k=1}^{\infty} e^{-\lambda_k t}, \ t > 0.$$
 (1.5)

This converges absolutely and uniformly on $[T, \infty)$ for any T > 0. Indeed, while $h_{\Omega}(t) \uparrow \infty$ as $t \downarrow 0$, the large-time behaviour is exponentially small apart from the possible contribution of a zero eigenvalue. More precisely, fix any T > 0. Then, in the Dirichlet case we have $\lambda_1 > 0$, hence by Weyl's law (1.3) there is a C > 0 such that

$$h_{\Omega}(t) \le Ce^{-\lambda_1 t}, \ t \ge T.$$
 (1.6)

In the Neumann case we instead have

$$h_{\Omega}(t) \le 1 + Ce^{-\lambda_2 t}, \ t \ge T \tag{1.7}$$

for some C > 0, assuming Ω is connected. In either case, Weyl's law (1.3) implies that

$$h_{\Omega}(t) \sim \frac{|\Omega|}{(4\pi t)^{n/2}}, \ t \downarrow 0.$$
 (1.8)

Since the heat trace (1.5) depends only on the spectrum, the same is true for any geometric quantity appearing in its asymptotic expansion as $t \downarrow 0$. In particular, (1.8) shows that both the volume and dimension of a domain are determined by the spectrum. We say that they are spectral invariants. This naturally raises the question: What other geometric quantities are and are not spectral invariants? For smoothly bounded planar domains, Pleijel (Pleijel, 1954) refined the heat trace asymptotics using Green's functions and methods due to Carleman to show that

$$h_{\Omega}(t) \sim \frac{|\Omega|}{4\pi t} - \frac{|\partial\Omega|}{8\sqrt{\pi t}}, \ t \downarrow 0.$$

In 1967, McKean and Singer (McKean Jr and Singer, 1967) extended this further by obtaining a third topological term in the expansion. By relating the heat trace coefficients to the curvature tensor and carefully manipulating certain Levi sums, they showed that

$$h_{\Omega}(t) \sim \frac{|\Omega|}{4\pi t} - \frac{|\partial\Omega|}{8\sqrt{\pi t}} + \frac{\chi(\Omega)}{6}, \ t \downarrow 0.$$
 (1.9)

This implies that, in addition to the area and perimeter, the Euler characteristic, or more intuitively the number of holes, is a spectral

invariant for smooth planar domains. One may even ask whether all of the geometry is a spectral invariant, that is, whether two domains or Riemannian manifolds that have the same eigenvalues must in fact be isometric. In 1964, Milnor gave a negative answer for Riemannian manifolds by constructing a pair of non-isometric 16-dimensional flat tori that are *isospectral*, i.e. have the same eigenvalues (Milnor, 1964). In 1966, Kac posed the analogous question for planar domains with Dirichlet boundary conditions, famously phrased as "Can one hear the shape of a drum?" This question remained open until 1992, when Gordon, Webb, and Wolpert constructed explicit examples of two isospectral non-isometric planar domains (Gordon et al., 1992).

These results show that the spectrum encodes some, but not all, geometric information, and the challenge lies in understanding precisely what can and cannot be heard from it. This thesis contributes to this broader theme through a sequence of studies that connect classical questions with new results. Chapter 2 is devoted to integrable polygons. Here we analyze the heat trace expansion and prove that, for this class, the length of the shortest closed geodesic is a spectral invariant. We also compute the spectral zeta function and its derivative at zero for the integrable polygons, and compare with known results. Finally, we study how the heat trace coefficients behave under geometric limits, in particular when smooth domains converge to polygons (not necessarily integrable) and vice versa. In Chapter 3 we turn to flat tori, presenting the first example of a 6-dimensional isospectral non-isometric triplet. In Chapter 4 we return to polygons, this time focusing on Neumann boundary conditions. We use locality principles to obtain an explicit estimate for the remainder term after the first three heat trace coefficients, which was previously only known for Dirichlet boundary conditions. Chapter 5 concludes the thesis with a summary of the main results and a discussion of possible directions for future research.

1.1 Main results of Paper 1

Paper 1 gives an overview of the historical and mathematical development of spectral geometry from Weyl's law in 1912 to today. We begin with a detailed proof of Weyl's law (1.3) for bounded domains with piecewise smooth boundary and Dirichlet boundary conditions, following Weyl's original proof of covering the domain by Euclidean boxes. We then focus on flat tori, introducing lattices and quadratic forms and explaining how the isospectral problem can be equivalently formulated in these settings. A highlight is Milnor's construction of a pair of non-isometric but isospectral flat tori in 16 dimensions, for which we explain the proof of both isospectrality and non-isometry. This part of Paper 1 concludes with a historical overview of the research of quadratic forms during the time between Weyl's law and Milnor's breakthrough.

Next, Paper 1 is devoted to Kac's famous question, "Can one hear the shape of a drum?". Although Kac's original arguments are heuristic and non-rigorous, we carefully explain the ideas and provide precise formulations. In particular, we establish a result that Kac was aiming for: If a sequence of convex polygonal domains converges in the Hausdorff sense to a smoothly bounded convex domain, then the third heat trace coefficient of the polygons converges to 1/6, which coincides with the third heat trace coefficient of the smooth domain. This analysis clarifies and makes rigorous the mathematical content underlying Kac's arguments.

Finally, Paper 1 ends with an overview of the evolution of spectral geometry in the decades following Kac's work, highlighting key advances and open questions that continue to drive the field today.

Chapter 2

Spectral invariants of integrable polygons

A polygonal domain is called *integrable* if every interior angle has the form $\frac{\pi}{m}$ for integers $m \geq 2$. Such a polygon is necessarily convex, and if we denote its interior angles by $\frac{\pi}{m_1}, \ldots, \frac{\pi}{m_n}$, then we have

$$\pi(n-2) = \sum_{k=1}^{n} \frac{\pi}{m_k} \le \frac{\pi n}{2}.$$

Thus, $n \le 4$, so n = 3 or n = 4. If n = 4, then it follows immediately that $m_k = 2$ for every $k = 1, \ldots, 4$. If instead n = 3, then we have

$$1 = \frac{1}{m_1} + \frac{1}{m_2} + \frac{1}{m_3},$$

and it is straightforward to verify that the only integer solutions up to permutation are $(m_1, m_2, m_3) = (3, 3, 3), (2, 4, 4),$ and (2, 3, 6). This shows that the integrable polygons are precisely rectangles, equilateral triangles, isosceles right triangles, and hemi-equilateral (30-60-90) triangles. The terminology "integrable" originates from the study of billiard dynamics, see (Gutkin, 1986).

One reason integrable polygons are interesting is that they are precisely the polygons that strictly tessellate the plane by reflections

across their sides (McCartin, 2008) (Rowlett et al., 2021). Recall that a polygon tessellating the plane by reflections means that, starting from a single copy of the polygon and reflecting it across its edges, one obtains a covering of the entire plane without overlaps or gaps. Such a tesselation is called *strict* if any line containing an edge of one of the reflected copies never intersects the interior of any copy. See (Rowlett et al., 2021, Def. 2) for a precise definition in \mathbb{R}^n . Although the regular hexagons are well known to tesselate the plane, this tesselation is not strict, since any line passing through one of their edges also intersects the interior of other hexagons.

Another reason integrable polygons are interesting is that we have explicit expressions for their Laplace eigenvalues with either Dirichlet or Neumann boundary conditions. Indeed, the rectangle $(0, a) \times (0, b)$, the equilateral triangle with side length ℓ , the isosceles right triangle with legs of length a, and the hemi-equilateral triangle with length of hypotenuse ℓ , respectively have the Dirichlet eigenvalues

$$\lambda_{m,n}^{\square} = \pi^2 \left(\frac{m^2}{a^2} + \frac{n^2}{b^2} \right), \ m, n > 0,$$

$$\lambda_{m,n}^{\nabla} = \frac{16\pi^2}{9\ell^2} (m^2 + mn + n^2), \ m, n > 0,$$

$$\lambda_{m,n}^{\diamondsuit} = \frac{\pi^2}{a^2} (m^2 + n^2), \ m > n > 0,$$

$$\lambda_{m,n}^{\heartsuit} = \frac{16\pi^2}{9\ell^2} (m^2 + mn + n^2), \ m > n > 0.$$
(2.1)

In all four cases, the Neumann eigenvalues are obtained by replacing the strict inequalities for m and n by \geq . Using (2.1), we can obtain explicit expressions for the spectral zeta functions and the heat traces, which will be done in the next sections.

2.1 Spectral zeta function

Let $\Omega \subset \mathbb{R}^n$ be a bounded domain with Dirichlet boundary conditions. Then the Laplacian has discrete spectrum (Levitin et al., 2023,

Thm. 2.1.28), and we define the *spectral zeta function* as the spectral invariant

$$\zeta(s) = \sum_{\lambda} \lambda^{-s},\tag{2.2}$$

where the sum goes through all eigenvalues counting multiplicity. The spectral zeta function, and in particular the associated spectral determinant, play a central role in spectral geometry and mathematical physics (see e.g. (Aurell and Salomonson, 1994) (Aldana and Rowlett, 2018)). To see how the spectral determinant and the spectral zeta function are related, recall from linear algebra that the determinant of a square matrix is equal to the product of its eigenvalues. Then, if we formally differentiate (2.2) termwise and insert s = 0, we obtain

$$\zeta'(0) = -\sum_{\lambda} \log(\lambda), \quad e^{-\zeta'(0)} = \prod_{\lambda} \lambda. \tag{2.3}$$

This suggests that we can think of $e^{-\zeta'(0)}$ as the determinant of the Laplacian. Of course, the right hand sides of (2.3) diverge. In fact, using Weyl's law (1.3), it is straightforward to verify that the sum in (2.2) converges for $s \in \mathbb{C}$ if and only if Re(s) > n/2, and is analytic for such s. Nevertheless, just as for the Riemann zeta function

$$\zeta_R(s) = \sum_{k=1}^{\infty} k^{-s},$$

one can show that $\zeta(s)$ defined by (2.2) has a meromorphic continuation to \mathbb{C} which is analytic at s=0 (Ray and Singer, 1971). In particular, $\zeta'(0)$ is well defined, and using (2.3) as motivation, we define the spectral determinant as $e^{-\zeta'(0)}$. This regularized determinant has important applications: it appears in functional integrals in quantum field theory, in formulas for the partition function of random surfaces, and in conformal geometry where it encodes how eigenvalues transform under changes of the metric (Ray and Singer, 1971) (Aurell and Salomonson, 1994).

In Paper 2 we use (2.1) to explicitly compute $\zeta'(0)$ for the integrable polygons. The result is the following.

Theorem 2.1.1. Let $\zeta_{\square}(s), \zeta_{\nabla}(s), \zeta_{\diamondsuit}(s), \zeta_{\diamondsuit}(s)$ denote the spectral zeta functions for the rectangle $(0, a) \times (0, b)$, the equilateral triangle with side length ℓ , the isosceles right triangle with legs of length a, and the hemi-equilateral triangle with length of hypotenuse ℓ , respectively, all with Dirichlet boundary conditions. Then we have

$$\zeta_{\square}'(0) = \frac{1}{2}\log(b) + \frac{1}{2}\log(2) + \frac{\pi a}{12b} + \sum_{n=1}^{\infty} \frac{1}{ne^{2\pi na/b}} \sum_{d|n} d,$$

$$\zeta_{\nabla}'(0) = \frac{2}{3}\log(\ell) + \frac{2}{3}\log(3) - \frac{2}{3}\log(2) + \frac{\pi\sqrt{3}}{36} + \frac{2}{3}\sum_{n=1}^{\infty} \frac{(-1)^n}{ne^{\pi n\sqrt{3}}} \sum_{d|n} d,$$

$$\zeta'_{\diamondsuit}(0) = \frac{3}{4}\log(a) + \frac{1}{2}\log(2) + \frac{\pi}{24} + \frac{1}{2}\sum_{n=1}^{\infty} \frac{1}{ne^{2\pi n}} \sum_{d|n} d,$$

$$\zeta_{\heartsuit}'(0) = \frac{5}{6}\log(\ell) + \frac{7}{12}\log(3) - \frac{5}{6}\log(2) + \frac{\pi\sqrt{3}}{72} + \frac{1}{3}\sum_{n=1}^{\infty} \frac{(-1)^n}{ne^{\pi n\sqrt{3}}} \sum_{d|n} d.$$

We explain briefly how to prove Theorem 2.1.1 and refer to Paper 2 for details. First, we use (Chowla and Selberg, 1949, p. 87) to write

$$\zeta_{\square}(s) = \frac{1}{2} \left(\frac{b}{\pi} \right)^{2s} \left[-\zeta_{R}(2s) + \frac{a\sqrt{\pi}}{b} \frac{\zeta_{R}(2s-1)\Gamma(s-1/2)}{\Gamma(s)} \right] + \left(\frac{ab}{\pi} \right)^{s} \frac{1}{\Gamma(s)} \sqrt{\frac{a}{b}} \sum_{n=1}^{\infty} n^{s-1/2} \sum_{d|n} d^{1-2s} \int_{0}^{\infty} x^{s-3/2} e^{-\pi an(x+x^{-1})/b} dx,$$

$$\zeta_{\nabla}(s) = \frac{1}{6} \left(\frac{3\ell}{4\pi} \right)^{2s} \left[-4\zeta_R(2s) + \frac{2^{2s}\sqrt{\pi}\zeta_R(2s-1)\Gamma(s-1/2)}{\Gamma(s)3^{s-1/2}} + \frac{4\pi^s 2^{s-1/2}}{\Gamma(s)3^{s/2-1/4}} \sum_{n=1}^{\infty} n^{s-1/2} \sum_{d|n} d^{1-2s} (-1)^n \int_0^{\infty} x^{s-3/2} e^{-\pi n\sqrt{3}(x+x^{-1})/2} dx \right],$$

11

$$\zeta_{\diamondsuit}(s) = -\frac{1}{4} \left(\frac{a}{\pi}\right)^{2s} \zeta_{R}(2s) - \frac{1}{2^{s+1}} \left(\frac{a}{\pi}\right)^{2s} \zeta_{R}(2s)
+ \frac{\sqrt{\pi}}{4} \left(\frac{a}{\pi}\right)^{2s} \frac{\zeta_{R}(2s-1)\Gamma(s-1/2)}{\Gamma(s)}
+ \frac{1}{2} \left(\frac{a^{2}}{\pi}\right)^{s} \frac{1}{\Gamma(s)} \sum_{n=1}^{\infty} n^{s-1/2} \sum_{d|n} d^{1-2s} \int_{0}^{\infty} x^{s-3/2} e^{-\pi n(x+x^{-1})} dx,$$

$$\zeta_{\odot}(s) = \frac{1}{12} \left(\frac{3\ell}{4\pi} \right)^{2s} \left[-4\zeta_R(2s) - \frac{6}{3^s} \zeta_R(2s) + \frac{2^{2s} \sqrt{\pi} \zeta_R(2s-1) \Gamma(s-1/2)}{\Gamma(s) 3^{s-1/2}} + \frac{4\pi^s 2^{s-1/2}}{\Gamma(s) 3^{s/2-1/4}} \sum_{n=1}^{\infty} n^{s-1/2} \sum_{d|n} d^{1-2s} (-1)^n \int_0^{\infty} x^{s-3/2} e^{-\pi n \sqrt{3}(x+x^{-1})/2} dx \right].$$

In the analytic continuation, the identities hold for all $s \in \mathbb{C} \setminus \{1\}$. Next, we differentiate these expressions with respect to s, justifying termwise differentiation of the series as well as differentiation under the integral signs. Then, we insert s = 0 and use that $\Gamma(s)$ has a simple pole at s = 0 with residue 1, in combination with the classical special values of the Riemann zeta function

$$\zeta_R(0) = -\frac{1}{2}, \ \zeta_R'(0) = -\frac{\log(2\pi)}{2}, \ \zeta_R(-1) = -\frac{1}{12},$$
(2.4)

to obtain the formulas in Theorem 2.1.1. Using the Dedekind eta function

$$\eta(\tau) = q^{1/12} \prod_{n=1}^{\infty} (1 - q^{2n}), \ q = e^{\pi i \tau}, \ \text{Im}(\tau) > 0,$$

we also obtain the equivalent expressions

$$\zeta'_{\square}(0) = \frac{1}{2} \log \left(\frac{2b}{|\eta(z_1)|^2} \right), \quad z_1 = \frac{ai}{b},
\zeta'_{\nabla}(0) = \frac{2}{3} \log \left(\frac{3\ell}{2|\eta(z_2)|} \right), \quad z_2 = \frac{-3 + i\sqrt{3}}{2},
\zeta'_{\diamondsuit}(0) = \frac{1}{4} \log \left(\frac{4a^3}{|\eta(i)|^2} \right),
\zeta'_{\heartsuit}(0) = \frac{1}{3} \log \left(\frac{3\ell}{2|\eta(z_2)|} \right) + \frac{1}{4} \log \left(\frac{3\ell^2}{4} \right).$$

In (Aurell and Salomonson, 1994), they use different methods to compute the spectral zeta functions of integrable polygons, expressing them in terms of the *L*-functions

$$L_3(s) = 1 - 2^{-s} + 4^{-s} - 5^{-s} + \dots,$$

$$L_4(s) = 1 - 3^{-s} + 5^{-s} - 7^{-s} + \dots$$

More precisely, they obtain

$$\zeta_{\square}(s) = \left(\frac{\pi}{a}\right)^{-2s} (L_4(s)\zeta_R(s) - \zeta_R(2s)) \text{ for } a = b,
\zeta_{\nabla}(s) = \frac{1}{2} \left(\frac{4\pi}{3\ell}\right)^{-2s} (L_3(s)\zeta_R(s) - \zeta_R(2s)),
\zeta_{\diamondsuit}(s) = \frac{1}{2} \left(\frac{\pi}{a}\right)^{-2s} (L_4(s)\zeta_R(s) - (1+2^{-s})\zeta_R(2s)),
\zeta_{\heartsuit}(s) = \frac{1}{2} \left(\frac{4\pi}{3\ell}\right)^{-2s} (L_3(s)\zeta_R(s) - (1+3^{-s})\zeta_R(2s)).$$

Using these, they derive

$$\zeta_{\square}'(0) = \frac{1}{4} \log(a^2) + \frac{1}{4} \log\left(\pi 2^5 \frac{\Gamma(3/4)^2}{\Gamma(1/4)^2}\right) \text{ for } a = b,
\zeta_{\nabla}'(0) = \frac{1}{3} \log\left(\frac{\text{Area}}{A(1/3, 1/3, 1/3)}\right) + \log\left(\frac{\Gamma(1/3)^{1/2} \pi^{1/2} 3^{2/3} 2^{-1/6}}{\Gamma(2/3)^{1/2}}\right),
\zeta_{\diamondsuit}'(0) = \frac{3}{8} \log\left(\frac{\text{Area}}{A(1/2, 1/4, 1/4)}\right) + \log\left(\frac{\Gamma(1/4)^{1/2} \pi^{1/2} 2^{7/8}}{\Gamma(3/4)^{1/2}}\right),
\zeta_{\heartsuit}'(0) = \frac{5}{12} \log\left(\frac{\text{Area}}{A(1/2, 1/3, 1/6)}\right) + \log\left(\frac{\Gamma(1/3) \pi^{1/2} 3^{11/24} 2^{2/9}}{\Gamma(2/3)}\right),
(2.5)$$

where Area is the area of the respective polygon, and

$$A(\alpha_0, \alpha_1, \alpha_\infty) = \frac{\pi}{2} \frac{\Gamma(\alpha_0) \Gamma(\alpha_1) \Gamma(\alpha_\infty)}{\Gamma(1 - \alpha_0) \Gamma(1 - \alpha_1) \Gamma(1 - \alpha_\infty)}.$$

We have compared Theorem 2.1.1 with (2.5) and found that they all coincide.

2.2 Heat trace expansion

Let Ω be an *n*-sided polygon (not necessarily integrable) with interior angles $\gamma_1, \ldots, \gamma_n$. In (van den Berg and Srisatkunarajah, 1988) it is shown that under Dirichlet boundary conditions, the heat trace $h_{\Omega}^D(t)$ admits the short time asymptotic expansion

$$h_{\Omega}^{D}(t) = \frac{|\Omega|}{4\pi t} - \frac{|\partial\Omega|}{8\sqrt{\pi t}} + \sum_{i=1}^{n} \frac{\pi^{2} - \gamma_{i}^{2}}{24\pi\gamma_{i}} + \mathcal{O}(e^{-c/t}), \ t \downarrow 0,$$
 (2.6)

for some c > 0 that they estimate in terms of the geometry of the polygon. Under Neumann boundary conditions, the heat trace $h_{\Omega}^{N}(t)$ is known to admit a similar expansion (Kokotov, 2009, Thm. 1) (Fursaev, 1994),

$$h_{\Omega}^{N}(t) = \frac{|\Omega|}{4\pi t} + \frac{|\partial\Omega|}{8\sqrt{\pi t}} + \sum_{i=1}^{n} \frac{\pi^{2} - \gamma_{i}^{2}}{24\pi\gamma_{i}} + \mathcal{O}(e^{-c/t}), \ t \downarrow 0.$$
 (2.7)

In Paper 4, we obtain the first estimate for c in the Neumann case. A natural question, both for Dirichlet and Neumann boundary conditions, is to determine the optimal (maximal) value of c. For general polygons this remains open. However, for integrable polygons the eigenvalue formulas (2.1) make it possible to compute the heat trace explicitly. This in turn allows us not only to verify the expansions (2.6), (2.7), but also to determine the optimal value of c in each case. Our result is the following.

Theorem 2.2.1. Let $h_{\square}^{D,N}(t), h_{\nabla}^{D,N}(t), h_{\diamondsuit}^{D,N}(t), h_{\heartsuit}^{D,N}(t)$ denote the heat traces for the rectangle $(0,a) \times (0,b)$, the equilateral triangle with side length ℓ , the isosceles right triangle with legs of length a, and the hemi-equilateral triangle with length of hypotenuse ℓ , respectively, with either

Dirichlet or Neumann boundary conditions. Then we have

$$\begin{split} h^{D,N}_{\square}(t) &= \frac{ab}{4\pi t} \pm \frac{a+b}{4\sqrt{\pi t}} + \frac{1}{4} + \mathcal{O}(t^{-1}e^{-\min(a,b)^2/t}), \ t \downarrow 0, \\ h^{D,N}_{\nabla}(t) &= \frac{\ell^2\sqrt{3}}{16\pi t} \pm \frac{3\ell}{8\sqrt{\pi t}} + \frac{1}{3} + \mathcal{O}(t^{-1/2}e^{-9\ell^2/(16t)}), \ t \downarrow 0, \\ h^{D,N}_{\diamondsuit}(t) &= \frac{a^2}{8\pi t} \pm \frac{a(2+\sqrt{2})}{8\sqrt{\pi t}} + \frac{3}{8} + \mathcal{O}(t^{-1/2}e^{-a^2/(2t)}), \ t \downarrow 0, \\ h^{D,N}_{\heartsuit}(t) &= \frac{\ell^2\sqrt{3}}{32\pi t} \pm \frac{\ell(3+\sqrt{3})}{16\sqrt{\pi t}} + \frac{5}{12} + O(t^{-1/2}e^{-3\ell^2/(16t)}), \ t \downarrow 0, \end{split}$$

where the minus sign corresponds to Dirichlet boundary conditions and the plus sign to Neumann boundary conditions. In all cases the remainders are sharp.

The key to proving Theorem 2.2.1 is to combine the explicit expressions for the eigenvalues (2.1) with Poisson's summation formula, which says that

$$\sum_{m \in \mathbb{Z}} f(x+m) = \sum_{m \in \mathbb{Z}} \hat{f}(m)e^{2\pi i mx}$$
 (2.8)

for any Schwartz function $f \in \mathcal{S}(\mathbb{R})$. Here, \hat{f} is the Fourier transform

$$\hat{f}(y) = \int_{\mathbb{R}} f(x)e^{-2\pi iyx} dx.$$

Letting x = 0 in (2.8) gives

$$\sum_{m \in \mathbb{Z}} f(m) = \sum_{m \in \mathbb{Z}} \hat{f}(m).$$

Applying this to $f(x) = e^{-ax^2}$ for a > 0, one obtains the identities

$$\sum_{m \in \mathbb{Z}} e^{-am^2} = \sqrt{\frac{\pi}{a}} \sum_{m \in \mathbb{Z}} e^{-\pi^2 m^2/a},$$
$$\sum_{m \in \mathbb{Z}} e^{-a(m+1/2)^2} = \sqrt{\frac{\pi}{a}} \sum_{m \in \mathbb{Z}} (-1)^m e^{-\pi^2 m^2/a},$$

which imply

$$\sum_{m=1}^{\infty} e^{-am^2} = \frac{1}{2} \left(\sqrt{\frac{\pi}{a}} - 1 \right) + \sqrt{\frac{\pi}{a}} \sum_{m=1}^{\infty} e^{-\pi^2 m^2 / a},$$

$$\sum_{m=1}^{\infty} e^{-a(m+1/2)^2} = \frac{1}{2} \left(\sqrt{\frac{\pi}{a}} - 2e^{-a/4} \right) + \sqrt{\frac{\pi}{a}} \sum_{m=1}^{\infty} (-1)^m e^{-\pi^2 m^2 / a}.$$
(2.9)

This gives the Dirichlet heat trace for the rectangle

$$h_{\square}^{D}(t) = \sum_{m=1}^{\infty} \sum_{n=1}^{\infty} e^{-\pi^{2}(m^{2}/a^{2} + n^{2}/b^{2})t} = \sum_{m=1}^{\infty} e^{-\pi^{2}m^{2}t/a^{2}} \sum_{n=1}^{\infty} e^{-\pi^{2}n^{2}t/b^{2}}$$

$$= \left(\frac{1}{2} \left(\frac{a}{\sqrt{\pi t}} - 1\right) + \frac{a}{\sqrt{\pi t}} \sum_{m=1}^{\infty} e^{-m^{2}a^{2}/t}\right)$$

$$\cdot \left(\frac{1}{2} \left(\frac{b}{\sqrt{\pi t}} - 1\right) + \frac{b}{\sqrt{\pi t}} \sum_{n=1}^{\infty} e^{-n^{2}b^{2}/t}\right)$$

$$= \frac{ab}{4\pi t} - \frac{a+b}{4\sqrt{\pi t}} + \frac{1}{4} + \frac{ab}{2\pi t} \sum_{m=1}^{\infty} e^{-m^2 a^2/t} + \frac{ab}{2\pi t} \sum_{n=1}^{\infty} e^{-n^2 b^2/t}$$

$$- \frac{a}{2\sqrt{\pi t}} \sum_{m=1}^{\infty} e^{-m^2 a^2/t} - \frac{b}{2\sqrt{\pi t}} \sum_{n=1}^{\infty} e^{-n^2 b^2/t} + \frac{ab}{\pi t} \sum_{m=1}^{\infty} \sum_{n=1}^{\infty} e^{-(m^2 a^2 + n^2 b^2)/t}.$$

Similarly, we obtain

$$h_{\nabla}^{D}(t) = \frac{\ell^{2}\sqrt{3}}{16\pi t} - \frac{3\ell}{8\sqrt{\pi t}} + \frac{1}{3} - \frac{3\ell}{4\sqrt{\pi t}} \sum_{m=1}^{\infty} e^{-9\ell^{2}m^{2}/(16t)} + \frac{\ell^{2}\sqrt{3}}{8\pi t} \sum_{n=1}^{\infty} e^{-3\ell^{2}n^{2}/(4t)} + \frac{\ell^{2}\sqrt{3}}{4\pi t} \sum_{m=1}^{\infty} \sum_{n=1}^{\infty} \sum_{n=1}^{\infty} e^{-3\ell^{2}(3m^{2}+n^{2})/(4t)} + \frac{\ell^{2}\sqrt{3}}{4\pi t} \sum_{m=1}^{\infty} \sum_{n=1}^{\infty} \sum_{n=1}^{\infty} e^{-3\ell^{2}(3(2m-1)^{2}+(2n-1)^{2})/(16t)},$$

$$h_{D(t)} = a^{2} - a(2+\sqrt{2}) - 3 - a - \sum_{m=1}^{\infty} e^{-3\ell^{2}/(2t)} = a^{2} - \sum_{m=1}^{\infty} e^{-m^{2}a^{2}/(2t)} = a^{2} - \sum_{m=1}^{\infty} e^{-$$

$$h_{\diamondsuit}^{D}(t) = \frac{a^{2}}{8\pi t} - \frac{a(2+\sqrt{2})}{8\sqrt{\pi t}} + \frac{3}{8} - \frac{a}{2\sqrt{2\pi t}} \sum_{m=1}^{\infty} e^{-m^{2}a^{2}/(2t)} + \frac{a^{2}}{2\pi t} \sum_{m=1}^{\infty} e^{-m^{2}a^{2}/t} - \frac{a}{2\sqrt{\pi t}} \sum_{m=1}^{\infty} e^{-m^{2}a^{2}/t} + \frac{a^{2}}{2\pi t} \left(\sum_{m=1}^{\infty} e^{-m^{2}a^{2}/t} \right)^{2},$$

$$\begin{split} h_{\heartsuit}^{D}(t) &= \frac{\ell^{2}\sqrt{3}}{32\pi t} - \frac{\ell(3+\sqrt{3})}{16\sqrt{\pi t}} + \frac{5}{12} - \frac{\ell}{8}\sqrt{\frac{3}{\pi t}} \sum_{m=1}^{\infty} e^{-3\ell^{2}m^{2}/(16t)} \\ &- \frac{3\ell}{8\sqrt{\pi t}} \sum_{m=1}^{\infty} e^{-9\ell^{2}m^{2}/(16t)} + \frac{\ell^{2}\sqrt{3}}{16\pi t} \sum_{n=1}^{\infty} e^{-3\ell^{2}n^{2}/(4t)} \\ &+ \frac{\ell^{2}\sqrt{3}}{16\pi t} \sum_{m=1}^{\infty} e^{-9\ell^{2}m^{2}/(4t)} + \frac{\ell^{2}\sqrt{3}}{8\pi t} \sum_{m=1}^{\infty} \sum_{n=1}^{\infty} e^{-3\ell^{2}(3m^{2}+n^{2})/(4t)} \\ &+ \frac{\ell^{2}\sqrt{3}}{8\pi t} \sum_{m=1}^{\infty} \sum_{n=1}^{\infty} e^{-3\ell^{2}(3(2m-1)^{2}+(2n-1)^{2})/(16t)}, \end{split}$$

which implies Theorem 2.2.1 in the Dirichlet case. In the Neumann case, Theorem 2.2.1 follows from noting that

$$\begin{split} h^N_\square(t) &= 1 + \sum_{n=1}^\infty e^{-\pi^2 n^2 t/b^2} + \sum_{m=1}^\infty e^{-\pi^2 m^2 t/a^2} + h^D_\square(t), \\ h^N_\nabla(t) &= 1 + 2 \sum_{m=1}^\infty e^{-16\pi^2 t/(9\ell^2)m^2} + h^D_\nabla(t), \\ h^N_\diamondsuit(t) &= 1 + \sum_{m=1}^\infty e^{-\pi^2 m^2 t/a^2} + \sum_{n=1}^\infty e^{-2\pi^2 n^2 t/a^2} + h^D_\diamondsuit(t), \\ h^N_\heartsuit(t) &= 1 + \sum_{m=1}^\infty e^{-\frac{16\pi^2}{9\ell^2}m^2 t} + \sum_{n=1}^\infty e^{-\frac{16\pi^2}{3\ell^2}n^2 t} + h^D_\heartsuit(t), \end{split}$$

and applying (2.9) to the extra sums that appear. See Paper 2 for details.

An interesting feature of Theorem 2.2.1 is the structure of the remainder terms. In each of the four integrable polygon cases, the exponent in the remainder can be chosen arbitrarily close to $L^2/4$, where L denotes the length of the shortest closed geodesic in the polygon. Indeed, by (Durso, 1988, p. 43) (Hezari et al., 2021, Prop. 8), the lengths of the shortest closed geodesics for the rectangle $(0, a) \times (0, b)$, the equilateral triangle with side length ℓ , the isosceles right triangle with legs of length a, and the hemi-equilateral triangle with length of hypotenuse ℓ are $2 \min(a, b)$, $3\ell/2$, $a\sqrt{2}$, and $\ell\sqrt{3}/2$, respectively. Thus, Theorem 2.2.1 can be equivalently formulated as follows.

Theorem 2.2.2. Let Ω be an integrable polygon with interior angles $\gamma_1, \ldots, \gamma_n$. Then, for any $\epsilon > 0$, the Dirichlet and Neumann heat traces satisfy

$$h_{\Omega}^{D,N}(t) = \frac{|\Omega|}{4\pi t} \pm \frac{|\partial\Omega|}{8\sqrt{\pi t}} + \sum_{i=1}^{n} \frac{\pi^{2} - \gamma_{i}^{2}}{24\pi\gamma_{i}} + \mathcal{O}(e^{-(L-\epsilon)^{2}/(4t)}), \ t \downarrow 0, \ (2.10)$$

where L denotes the length of the shortest closed geodesic in the polygon. The remainder is sharp in the sense that it does not hold for $\epsilon = 0$.

Theorem 2.2.2 makes it natural to conjecture that (2.10) holds for any convex polygon, and possibly even for non-convex polygons. This would, in particular, imply that the shortest closed geodesic is a spectral invariant for polygons. It is already known that the length of the shortest closed geodesic is a spectral invariant for triangular domains, proved using singularities of the wave trace by Durso (Durso, 1988). For general polygons, Durso proved that the Poisson relation holds, which implies that singularities of the wave trace may only occur at lengths of closed geodesics. However, it remains unknown whether the shortest closed geodesic necessarily generates a singularity in this trace, and hence it is an open problem whether this length is a spectral invariant for general polygons.

In Paper 2, we show that a remainder estimate similar to (2.10) holds for flat tori, and we conjecture similar remainders for arbitrary Euclidean space forms and polytopes in \mathbb{R}^n .

2.3 Convex polygons and smoothly bounded domains

In this section, we compare the heat trace expansion of smoothly bounded planar domains to that of polygonal domains that need not be integrable. We start by recalling the following result.

Proposition 2.3.1. Let $\Omega \subset \mathbb{R}^2$ be a smoothly bounded domain. For

Dirichlet boundary conditions, the heat trace of Ω satisfies

$$h_{\Omega}(t) \sim \frac{a_{-1}}{t} + \frac{a_{-1/2}}{\sqrt{t}} + a_0 + a_{1/2}\sqrt{t}, \ t \downarrow 0,$$

where

$$a_{-1} = \frac{|\Omega|}{4\pi}, \ a_{-1/2} = -\frac{|\partial\Omega|}{8\sqrt{\pi}},$$

$$a_{0} = \frac{1}{12\pi} \int_{\partial\Omega} k(s)ds, \ a_{1/2} = \frac{1}{256\sqrt{\pi}} \int_{\partial\Omega} k(s)^{2}ds,$$
(2.11)

with k(s) being the Gauss curvature of the boundary. If in addition Ω is convex, then $a_0 = 1/6$.

Proof. The formulas given by (2.11) can be found in (Watanabe, 2000). Moreover, by (Nursultanov et al., 2024, Thm. 6.10, Remark 6.15) we have $a_0 = \chi(\Omega)/6$, where $\chi(\Omega)$ is the Euler characteristic of Ω . This equals 1/6 if Ω is convex.

As a consequence, we will see that the first two heat trace coefficients of a sequence of smoothly bounded convex domains that converge to a convex polygonal domain converge to that of the polygonal domain. However, the third heat trace coefficient does *not* converge to that of the polygonal domain.

Theorem 2.3.2. Let $\{\Omega_k\}_{k\geq 1}$ be a sequence of convex smoothly bounded domains in \mathbb{R}^2 and let Ω be a convex polygon such that $\Omega_k \to \Omega$ in the Hausdorff distance. For Dirichlet boundary conditions, the heat trace coefficients satisfy

$$a_j(\Omega_k) \to a_j(\Omega), \quad j = -1, -1/2, \quad a_0(\Omega_k) \not\to a_0(\Omega).$$

Proof. With the assumptions of convexity and Hausdorff convergence, it follows that the areas $|\Omega_k|$ and perimeters $|\partial\Omega_k|$ converge to $|\Omega|$ and $|\partial\Omega|$, respectively. So we now consider the third heat trace coefficient. By Proposition 2.3.1, $a_0(\Omega_k) = 1/6$ for every k. We will show that

 $a_0(\Omega) > 1/6$, from which the result follows. If we denote the interior angles by $\gamma_1, \ldots, \gamma_n$, then by (2.6)

$$a_0(\Omega) = \sum_{i=1}^n \frac{\pi^2 - \gamma_i^2}{24\pi\gamma_i} = \frac{\pi}{24} \sum_{i=1}^n \frac{1}{\gamma_i} - \frac{1}{24\pi} \sum_{i=1}^n \gamma_i = \frac{\pi}{24} \sum_{i=1}^n \frac{1}{\gamma_i} - \frac{n-2}{24}.$$

By the Cauchy-Schwarz inequality,

$$n^{2} \le \sum_{i=1}^{n} \frac{1}{\gamma_{i}} \sum_{i=1}^{n} \gamma_{i} = \sum_{i=1}^{n} \frac{1}{\gamma_{i}} \pi(n-2),$$

so that

$$\sum_{i=1}^{n} \frac{1}{\gamma_i} \ge \frac{n^2}{\pi(n-2)}.$$

Thus,

$$a_0(\Omega) \ge \frac{\pi}{24} \frac{n^2}{\pi(n-2)} - \frac{n-2}{24} = \frac{1}{6} + \frac{1}{6(n-2)} > \frac{1}{6}.$$
 (2.12)

Using the notation of Theorem 2.3.2, it follows that

$$\lim_{k \to \infty} a_0(\Omega_k) \neq a_0 \bigg(\lim_{k \to \infty} \Omega_k \bigg).$$

In other words, the map $\Omega \to a_0(\Omega)$ is not continuous in the Hausdorff topology. Intuitively, this failure arises because the third heat trace coefficient encodes different geometric information in the smooth and polygonal cases. For smooth domains, it depends on the integrated boundary curvature, while for polygons, it depends on the interior angles at the corners. Although a sequence of smooth curves can approximate a corner arbitrarily well in shape, we cannot expect the curves to capture the singular corner contributions appearing in the polygonal coefficient. It is interesting to note that if instead we approximate a smoothly bounded domain by polygonal domains, this third heat trace coefficient of the polygonal domains converges to that of the smoothly bounded domain.

Theorem 2.3.3 (See Mårdby (2023), Thm. 4.4.1). Let $\{\Omega_k\}_{k\geq 1}$ be a sequence of N_k -sided convex polygons with interior angles $\gamma_{k,j}$, for $k\geq 1$ and $1\leq j\leq N_k$. Assume that $\overline{\Omega_k}\to \overline{\Omega}$ in Hausdorff, with Ω being a non-empty smoothly bounded convex domain. Then the first three Dirichlet heat trace coefficients of Ω_k converge to those of Ω .

Proof. The first two heat trace coefficients converge thanks to the assumptions of Hausdorff convergence and convexity. By (Mårdby and Rowlett, 2024, Lemma 4.7), the interior angles $\gamma_{k,j}$ all tend to π as the polygons tend to the smoothly bounded domain in Hausdorff convergence. Next, we show that $N_k \to \infty$ as $k \to \infty$. Suppose instead that there is an M>0 such that $N_k \leq M$ for all k. Since the angles all tend to π , there is an $N\geq 1$ such that $\gamma_{k,j}>\pi-\frac{2\pi}{M}$ for all $k\geq N$ and $1\leq j\leq N_k$. Then, for $k\geq N$,

$$\pi(N_k - 2) = \sum_{j=1}^{N_k} \gamma_{k,j} > N_k \left(\pi - \frac{2\pi}{M}\right),$$

which implies that $N_k > M$, a contradiction.

Now, the term a_0 for each k is

$$a_0(\Omega_k) = \frac{\pi}{24} \sum_{k=1}^{N_k} \frac{1}{\gamma_{k,j}} - \frac{N_k}{24} + \frac{1}{12}.$$

Following the proof of (Mårdby, 2023, Thm. 4.4.1), we can write $\gamma_{k,j} = \pi(1 - f(k,j)), k \ge 1, 1 \le j \le N_k$, from which it follows that $\sum_{j=1}^{N_k} f(k,j) = 2$ for every k and

$$a_0(\Omega_k) = \frac{1}{6} + \frac{1}{24} \sum_{j=1}^{N_k} \frac{f(k,j)^2}{1 - f(k,j)}.$$

If we then write

$$\epsilon_k = \max_{1 \le j \le N_k} f(k, j),$$

then $\epsilon_k \to 0$ because the angles tend to π . We therefore obtain that

$$0 \le \sum_{j=1}^{N_k} \frac{f(k,j)^2}{1 - f(k,j)} \le \frac{\epsilon_k}{1 - \epsilon_k} \sum_{j=1}^{N_k} f(k,j) = \frac{2\epsilon_k}{1 - \epsilon_k} \to 0 \text{ as } k \to \infty.$$

Thus,
$$a_0(\Omega_k) \to 1/6 = a_0(\Omega)$$
 as $k \to \infty$.

Chapter 3

Three's company in six dimensions

A flat torus is a compact Riemannian manifold obtained as a quotient of Euclidean space by a *full-rank lattice*. We recall here some fundamentals in the study of flat tori. Let A be an invertible $n \times n$ matrix with real-valued entries. A *full-rank lattice* is a set

$$L := A\mathbb{Z}^n = \{Ax : x \in \mathbb{Z}^n\}.$$

The matrix A is called a basis matrix for the lattice. It is not unique, but all basis matrices are related in the sense that every other basis matrix can be expressed as AB for some unimodular matrix B. Recall that B being unimodular means that it is invertible, has integer entries, and its inverse also has integer entries. For a full-rank lattice $L \subset \mathbb{R}^n$, there is an associated full-rank lattice known as the dual, defined as

$$L^* := \{ \ell \in \mathbb{R}^n : \ell \cdot \gamma \in \mathbb{Z} \text{ for all } \gamma \in L \}.$$

Using the identity $x \cdot (Ay) = (A^T x) \cdot y$, it is straightforward to show that if A is a basis matrix for L, then $(A^{-1})^T$ is a basis matrix for L^* . It is then a classical exercise to prove that the spectrum of the flat torus \mathbb{R}^n/L is the multiset

$$\{4\pi^2||\ell||^2: \ell \in L^*\},\$$

meaning that we count multiplicity. This shows that, to investigate the Laplace spectrum of a flat torus, it is equivalent to study the lengths of the vectors in full-rank lattices. The set of lengths of vectors in a full-rank lattice, counted with multiplicity, is known as its length spectrum. In this way, the study of the Laplace spectrum of the flat torus \mathbb{R}^n/L is equivalent to the study of the length spectrum of the dual lattice L^* . We may simply refer to this as the spectrum of the lattice, keeping in mind the equivalence between the Laplace spectrum of a flat torus and the length spectrum of the associated lattice.

A closely related object that is also useful not only for studying lattices but also for problems in number theory is a quadratic form. Given an n-dimensional full-rank lattice L with basis matrix A, let $Q = A^T A$. Then, we identify Q with the quadratic form that acts on $x \in \mathbb{R}^n$ via $Q(x) = x^T Q x$. If P is an $n \times n$ matrix with $B^T Q B = P$, for a unimodular matrix B, then we say that P is integrally equivalent to Q. Since any other basis matrix for L can be expressed as AB for a unimodular matrix B, we therefore associate the class of integrally equivalent quadratic forms with the lattice L. For $t \in \mathbb{R}$, the t-th representation number, often denoted R(Q,t), is the number of distinct $x \in \mathbb{Z}^n$ such that Q(x) = t. For the flat torus \mathbb{R}^n/L with L = t $A\mathbb{Z}^n$, there is a natural bijection between the length spectrum of L and the representation numbers of this equivalence class of quadratic forms. For $x \in \mathbb{Z}^n$, the length of the lattice vector ||Ax|| is mapped to $Q(x) = x^T A^T A x = ||Ax||^2$. In this way, one can also see that the representation numbers of integrally equivalent quadratic forms are identical. Consequently, two flat tori are isospectral if and only if the representation numbers of their associated equivalence classes of quadratic forms are identical.

It is then natural to ask, what does the Laplace spectrum of a flat torus say about its 'shape', and therewith the shape of the associated lattice? Equivalently, to what extent can we identify a quadratic form if we know its representation numbers? Perhaps the most fundamental question in this direction is: If two flat tori are isospectral, then are they isometric? Being isometric is equivalent to the existence of an orthogonal transformation that takes the first lattice to the second lattice. It is a classical exercise to prove that if two 1-dimensional flat tori are isospectral, then they are isometric. It takes slightly more work to prove that this also holds in two dimensions (see (Nilsson et al., 2023, Thm. 5.2)). The first example of two flat tori which are isospectral but *not* isometric is a 16-dimensional pair found by Milnor in 1964 (Milnor, 1964).

After Milnor's example was found, a question arose: What is the smallest dimension in which isospectral non-isometric flat tori exist? In 1967 Kneser found a 12-dimensional pair (Kneser, 1967). It took ten years for Kitaoka to find a pair in dimension 8 in 1977 (Kitaoka, 1977). 15 years later Conway and Sloane managed to find 6- and 5-dimensional examples (Conway and Sloane, 1992). In 1990, Schiemann used a computer to find a 4-dimensional example (Schiemann, 1990). One year later, Shiota found another 4-dimensional pair (Shiota, 1991), and in the same year Earnest and Nipp found yet another pair (Earnest and Nipp, 1991). In 1992, Conway and Sloane found an infinite family of 4-dimensional pairs (Conway and Sloane, 1992) (Cerviño and Hein, 2011). Then, in 1994 Schiemann showed, using an advanced computer algorithm now known as Schiemann's algorithm (Nilsson et al., 2023), that there are no pairs in three dimensions (Schiemann, 1994, 1997). Thus, the smallest dimension in which isospectral non-isometric flat tori exist is four.

Now, we may wonder, how many flat tori can share a common Laplace spectrum? In 1978, Wolpert showed that any collection of mutually isospectral non-isometric flat tori is finite (Wolpert, 1978). Suwa-Bier improved this result in 1984 by showing that the supremum over the sizes of all such collections in any given dimension is also finite (Suwa-Bier, 1984). However, it is not clear how to extract an explicit upper bound bound from (Wolpert, 1978; Suwa-Bier, 1984), and we are also unaware of a conjecture concerning the precise value of this supremum as a function of the dimension. As soon as one has pairs of isospectral non-isometric flat tori in a given dimension, one can begin constructing increasingly larger families of isospectral yet mutually non-isometric

flat tori. For instance, if (L_1, L_2) is Schiemann's 4-dimensional pair of incongruent, meaning they do not differ by orthogonal transformation, lattices with equal spectra, then

$$(L_1 \oplus L_1, L_1 \oplus L_2, L_2 \oplus L_2)$$
 (3.1)

is an 8-dimensional triplet of incongruent lattices with equal spectra. Here, \oplus denotes the direct sum of the canonical embeddings of the 4-dimensional lattices in the first four, respectively last four, coordinate directions of \mathbb{R}^8 . To the best of our knowledge, no such triplets have been demonstrated in dimensions lower than 8 - until now. We present for the first time a triplet of 6-dimensional mutually isospectral and non-isometric flat tori. We start by providing a high-level explanation of our search algorithm.

3.1 Search algorithm

The main idea here is to search for triplets among linear codes. Let q and n be positive integers. A linear code is a subgroup of the additive group $(\mathbb{Z}/q\mathbb{Z})^n$, and its elements are called codewords. Every linear code of $(\mathbb{Z}/q\mathbb{Z})^n$ has a so-called generator matrix, which is a (not unique) $n \times n$ matrix whose rows consist of generators of the subgroup. Since any subgroup can be generated by n or fewer elements of the group, in case the subgroup has less than n generators, a generator matrix will have some rows containing only zeros. For example, the subgroup consisting of only the identity element of the group has the generator matrix that is the $n \times n$ matrix with all entries equal to zero.

To understand the relationship between linear codes and integer lattices, we define the projection map $\pi_q: \mathbb{Z}^n \to (\mathbb{Z}/q\mathbb{Z})^n$ by $\pi_q(z) = z \mod q$. Here, mod q acts coordinate-wise and refers to the integers modulo q. For a lattice $L \subset \mathbb{Z}^n$, $\pi_q(L)$ is a linear code, and for a linear code C, $\pi_q^{-1}(C)$ is a lattice. Further, the following lemma shows that every lattice is the pre-image of at least one linear code.

27

Lemma 3.1.1 (Nilsson et al. (2023), Section 2.1 & 3.3). Let L be a full-rank lattice in \mathbb{Z}^n . Then $L = \pi_q^{-1}(\pi_q(L))$ if and only if $q\mathbb{Z}^n \subset L$. If $L = A\mathbb{Z}^n$, then $\det(A)\mathbb{Z}^n \subset L$.

As observed by Conway and Fung (Conway and Fung, 1997, p. 40–42), one can deduce isospectrality of lattices by looking at weight distributions of codes. We say that two linear codes have equal weight distributions if there is a bijection between codewords that preserves the codewords up to permutations and signs (modulo q). For q=2, this is equivalent to the bijection preserving the number of non-zero elements. It is straightforward to check that if C_1 and C_2 are linear codes in $(\mathbb{Z}/q\mathbb{Z})^n$ with equal weight distributions, then $\pi_q^{-1}(C_i)$, i=1,2 are isospectral lattices (see (Nilsson et al., 2023, Prop. 3.12)). For each qand n, the set of linear codes is finite. One can therefore use an algorithm as described in Figure 3.1 to search for isospectral non-isometric flat tori. The algorithm guarantees that the flat tori corresponding to linear codes in the same equivalence class are isospectral, because the equivalence classes consist of codes with identical weight distributions. To check that the flat tori are not isometric, one can use Lemma 3.3.1, together with a computer program.

For q=5 and n=6 we found, using our algorithm, three linear codes C_1,C_2,C_3 with equal weight distributions. Their corresponding lattices are

$$L_{1} = \pi_{5}^{-1}(C_{1}) = \begin{bmatrix} 1 & 0 & 0 & 0 & 0 & 0 \\ 0 & 1 & 0 & 0 & 0 & 0 \\ 0 & 0 & 1 & 0 & 0 & 0 \\ 1 & 1 & 0 & 5 & 0 & 0 \\ 2 & 0 & 1 & 0 & 5 & 0 \\ 1 & 2 & 1 & 0 & 0 & 5 \end{bmatrix} \mathbb{Z}^{6},$$

$$L_{2} = \pi_{5}^{-1}(C_{2}) = \begin{bmatrix} 1 & 0 & 0 & 0 & 0 & 0 \\ 0 & 1 & 0 & 0 & 0 & 0 \\ 0 & 0 & 1 & 0 & 0 & 0 \\ 2 & 1 & 0 & 5 & 0 & 0 \\ 0 & 1 & 1 & 0 & 5 & 0 \\ 3 & 2 & 1 & 0 & 0 & 5 \end{bmatrix} \mathbb{Z}^{6},$$

$$L_{3} = \pi_{5}^{-1}(C_{3}) = \begin{bmatrix} 1 & 0 & 0 & 0 & 0 & 0 \\ 0 & 1 & 0 & 0 & 0 & 0 \\ 0 & 0 & 1 & 0 & 0 & 0 \\ 0 & 0 & 1 & 0 & 0 & 0 \\ 2 & 1 & 0 & 5 & 0 & 0 \\ 0 & 1 & 1 & 0 & 5 & 0 \\ 2 & 3 & 1 & 0 & 0 & 5 \end{bmatrix} \mathbb{Z}^{6}.$$
(3.2)

In the following sections, we will prove that these correspond to three mutually isospectral and non-isometric irreducible flat tori.

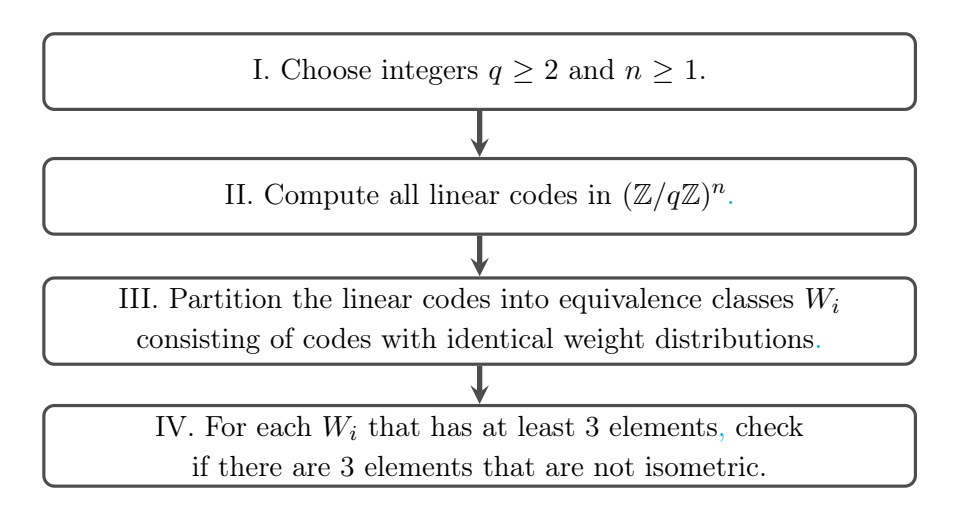


Figure 3.1: This is the search process we used to find our triplet.

3.2 Isospectrality

To show that the three lattices $L_i = A_i \mathbb{Z}^6$ in (3.2) correspond to three isospectral flat tori, we instead show the equivalent fact that the

29

quadratic forms

$$Q_{1} = A_{1}^{T} A_{1} = \begin{bmatrix} 7 & 3 & 3 & 5 & 10 & 5 \\ 3 & 6 & 2 & 5 & 0 & 10 \\ 3 & 2 & 3 & 0 & 5 & 5 \\ 5 & 5 & 0 & 25 & 0 & 0 \\ 10 & 0 & 5 & 0 & 25 & 0 \\ 5 & 10 & 5 & 0 & 0 & 25 \end{bmatrix},$$

$$Q_{2} = A_{2}^{T} A_{2} = \begin{bmatrix} 14 & 8 & 3 & 10 & 0 & 15 \\ 8 & 7 & 3 & 5 & 5 & 10 \\ 3 & 3 & 3 & 0 & 5 & 5 \\ 10 & 5 & 0 & 25 & 0 & 0 \\ 0 & 5 & 5 & 0 & 25 & 0 \\ 15 & 10 & 5 & 0 & 0 & 25 \end{bmatrix},$$

$$Q_{3} = A_{3}^{T} A_{3} = \begin{bmatrix} 9 & 8 & 2 & 10 & 0 & 10 \\ 8 & 12 & 4 & 5 & 5 & 15 \\ 2 & 4 & 3 & 0 & 5 & 5 \\ 10 & 5 & 0 & 25 & 0 & 0 \\ 0 & 5 & 5 & 0 & 25 & 0 \\ 10 & 15 & 5 & 0 & 0 & 25 \end{bmatrix}$$

$$(3.3)$$

have the same representation numbers. This can be done using the following result, which follows from Hecke's identity theorem for modular forms. Recall that a quadratic form Q is called *even* if every element in Q is an integer and the diagonal elements are even. If Q is even and positive definite, we define N_Q to be the smallest positive integer such that $N_Q Q^{-1}$ is even.

Theorem 3.2.1 ((Nilsson et al., 2023, Thm. 3.6)). Let P and Q be two even positive definite quadratic forms in 2k variables. Assume $\det(P) = \det(Q)$, $N_P = N_Q$, and that the t-th representation numbers of P and Q coincide for $0 \le t \le \mu_0(N_P)k/6 + 2$, where

$$\mu_0(N) = N \prod_{p|N, \ prime} \left(1 + \frac{1}{p}\right).$$
 (3.4)

Then all representation numbers for P and Q are the same.

We point out that a subtly misstated version of this result appears in (Nilsson et al., 2023, Cor. 3.7). The salient point is that to show that two even quadratic forms in 2k variables are isospectral, it is not enough to check that their representation numbers up to $\frac{\mu_0(N_P)k}{12} + 1$ are the same. Instead, one must check that the first $\frac{\mu_0(N_P)k}{12} + 1$ even representation numbers, i.e. the representation numbers up to $2(\frac{\mu_0(N_P)k}{12} + 1)$, are the same. The result can easily be extended to odd dimensions, as explained in (Nilsson et al., 2023, Section 3.2).

Theorem 3.2.2. The three quadratic forms Q_i given by (3.3) have the same representation numbers, hence the corresponding flat tori are isospectral.

Proof. While Q_i are not even, $2Q_i$ are, and Q_i have the same representation numbers if and only if $2Q_i$ do. Now, the reader may verify that $\det(2Q_i) = 10^6$ and $N_{2Q_i} = 100$, i = 1, 2, 3. Moreover, $\mu_0(100) = 180$ and $\mu_0(N_{2Q_i})3/6 + 2 = 92$, so it remains to show that $2Q_i$ have the same representation numbers up to 92. We have checked this with a well-tested computer program. The result is shown in Table 3.1.

Table 3.1: The representation numbers $R_i(t) := R_i(2Q_i, t)$ of $2Q_i$ for i = 1, 2, 3 and $t = 0, 2, 4, \ldots, 92$. Each column pair lists values of t and the corresponding $R_i(t)$, with $R_i(t)$ referring to the t-value in the column directly to its left.

t	$R_i(t)$										
0	1	16	8	32	30	48	54	64	160	80	200
2	0	18	4	34	34	50	70	66	112	82	132
4	0	20	12	36	46	52	68	68	110	84	220
6	2	22	16	38	52	54	120	70	184	86	366
8	2	24	22	40	48	56	124	72	108	88	202
10	2	26	18	42	28	58	64	74	162	90	170
12	2	28	20	44	78	60	104	76	230	92	236
14	10	30	32	46	102	62	124	78	164		

3.3 Non-isometry

Let $L_1 = A_1 \mathbb{Z}^n$ and $L_2 = A_2 \mathbb{Z}^n$ be two full-rank lattices in \mathbb{R}^n . The flat tori \mathbb{R}^n/L_1 and \mathbb{R}^n/L_2 are isometric as Riemannian manifolds if and only if the lattices L_1, L_2 are congruent, meaning that $CL_1 = L_2$ for some orthogonal matrix $C \in O_n(\mathbb{R})$. This holds if and only if the quadratic forms $Q_1 = A_1^T A_1$ and $Q_2 = A_2^T A_2$ are integrally equivalent. A convenient way to check whether two quadratic forms are integrally equivalent uses the following result, which is a version of (Nilsson et al., 2023, Cor. 3.3).

Lemma 3.3.1. Let Q_1, Q_2 be two positive definite n-dimensional quadratic forms. Let λ_{\min} be the smallest eigenvalue of Q_1 . If $B^TQ_1B = Q_2$ for some unimodular matrix B with columns b_j , then

$$b_i^T Q_1 b_j = (Q_2)_{ij}, \ i, j = 1, \dots, n.$$
 (3.5)

Moreover, $||b_i||^2 \le (Q_2)_{ij}/\lambda_{\min}$ for each $j = 1, \ldots, n$.

Since the elements in the unimodular matrix B are integers, there are only finitely many such matrices satisfying the conditions in Lemma 3.3.1.

Theorem 3.3.2. The three quadratic forms given by (3.3) are not integrally equivalent, hence the corresponding flat tori are non-isometric.

Proof. The smallest eigenvalue of Q_1 is $\lambda_{\min} \approx 0.7058$. Thus, if $B^T Q_1 B = Q_2$ for some unimodular matrix B with columns b_j , then by Lemma 3.3.1 we have

$$||b_1||^2 \le \frac{14}{\lambda_{\min}} \quad ||b_2||^2 \le \frac{7}{\lambda_{\min}}, \quad ||b_3||^2 \le \frac{3}{\lambda_{\min}}, ||b_4||^2 \le \frac{25}{\lambda_{\min}}, \quad ||b_5||^2 \le \frac{25}{\lambda_{\min}}, \quad ||b_6||^2 \le \frac{25}{\lambda_{\min}}.$$
(3.6)

However, using a well-tested computer program, we find that no such matrix B satisfies $b_i^T Q_1 b_j = (Q_2)_{ij}$ for all i, j. Therefore Q_1 and Q_2 are not integrally equivalent. The result follows similarly for Q_1, Q_3 and Q_2, Q_3 .

3.4 Irreducibility

A lattice L is called reducible if it is the orthogonal direct sum of two lower-dimensional lattices L_1 and L_2 (of dimensions at least one). We write this as $L = L_1 \oplus L_2$. If a lattice is not reducible, we say it is irreducible. We want to determine if our 6-dimensional triplet given by (3.2) consists of reducible or irreducible lattices. A motivation for this question is the fact that many of the examples of isospectral non-isometric flat tori have been produced using one reducible lattice and one irreducible lattice, including Milnor's 16-dimensional pair (Milnor, 1964) and Conway's 6-dimensional pair (Conway and Fung, 1997).

Theorem 3.4.1. The three lattices L_i given by (3.2) are irreducible.

Proof. We show that L_1 is irreducible. The proof for L_2 and L_3 is similar. Suppose L_1 is reducible, so that $L_1 = U \oplus V$ for some sublattices U and V of dimension less than six. Then every vector in U is orthogonal to every vector in V.

Now, using a computer, we find that the shortest non-zero vectors in L_1 are $v_1^{\pm} = \pm (0,0,1,0,1,1)$. For simplicity, we write v_1 to indicate v_1^+ , and use the analogous notation for v_i below for i=2,3,4,5,6 as well as w_4 . The vectors v_1^{\pm} are in either U or V since a sum of a non-zero vector in U and V has length strictly greater than $||v_1||$. Assuming $v_1 \in V$, we then note that the shortest non-zero vectors in L_1 apart from v_1^{\pm} are $v_2^{\pm} = \pm (1,0,-1,1,1,0)$. While v_1 and v_2 are orthogonal, they do in fact belong to the same sublattice V. To see this, note that the shortest non-zero vectors in L_1 apart from v_1^{\pm} and v_2^{\pm} are $v_3^{\pm} = \pm (0,1,-1,1,-1,1)$. If $v_1 \in V$ and $v_2 \in U$, then v_3 is neither in U nor in V since v_3 is not orthogonal to v_1 or v_2 . So, $v_3 = u' + v'$ for some $u' \in U$ and $v' \in V$. Then

$$5 = ||v_3||^2 = ||u'||^2 + ||v'||^2 \ge ||v_2||^2 + ||v_1||^2 = 7,$$
 (3.7)

which is a contradiction. It follows that both v_1 and v_2 are in V. Then v_3 is not in U, because it is not orthogonal to v_1 and v_2 . If it were a sum of non-zero elements in U and V, its length would be strictly

greater than the shortest vector in U. This is a contradiction, because this shortest vector is at least of length $||v_3||$. Therefore $v_3 \in V$.

Next, the shortest vectors in L_1 which are linearly independent of v_1, v_2, v_3 are $v_4^{\pm} = \pm(2, -1, 0, 1, -1, 0)$ and $w_4^{\pm} = \pm(1, -1, 1, 0, -2, 0)$. Since v_4, w_4 are not orthogonal to v_1 , it follows by the same argument as before that $v_4, w_4 \in V$. Similarly, the shortest vectors in L_1 linearly independent of v_1, v_2, v_3, v_4 are $v_5^{\pm} = \pm(1, 0, 1, 2, 1, -1)$, which again are in V because they are not orthogonal to v_1 . Finally, the shortest vectors in L_1 which are linearly independent of v_1, v_2, v_3, v_4, v_5 are $v_6^{\pm} = \pm(2, 1, 1, -2, 0, 0)$, which are also in V since they are not orthogonal to v_1 . Therefore, we have six linearly independent vectors in the same sublattice, which contradicts that the sublattice has dimension less than six. We conclude that no such sublattices of L_1 exist.

3.5 Choir numbers

For any $n \geq 1$, the *n*-th choir number \flat_n (Nilsson et al., 2023, Definition 5.1) is the maximum number k such that there exist k mutually isospectral and non-isometric n-dimensional flat tori. The name choir number is derived from the connection of Laplace spectra to music inspired by Kac's article Can one hear the shape of a drum? (Kac, 1966). In 1990-1994, Schiemann proved that $\flat_1 = \flat_2 = \flat_3 = 1$ and $\flat_n \geq 2$ for $n \geq 4$ (Schiemann, 1990, 1994). Now, let (L_1, L_2) be a pair of 4-dimensional incongruent and isospectral lattices. Then

$$L_{i_1\dots i_n} := 1 \cdot L_{i_1} \oplus 2 \cdot L_{i_2} \oplus \dots \oplus n \cdot L_{i_n}, \tag{3.8}$$

where $\lambda \cdot L$ denotes the scaling of the lattice L by the constant λ , are 4n-dimensional, incongruent, and isospectral for any $i_j \in \{1, 2\}$. The scalings are included to make sure that the lattices are incongruent, and they may be chosen arbitrarily as long as they are non-zero and distinct up to sign. Since they are 2^n in number, we conclude that $b_{4n} \geq 2^n$. Thus, the choir numbers grow faster than any polynomial. This argument can be generalized to show that the choir numbers are supermultiplicative. In other words, we have $b_{m+n} \geq b_m b_n$ for all

 $m, n \geq 1$. In particular, using our 6-dimensional triplet, we find that $b_6 \geq 3$ and $b_{6n} \geq 3^n$. In fact, by combining

$$\flat_{m+n} \ge \flat_m \flat_n, \quad \flat_4 \ge 2, \quad \flat_6 \ge 3, \tag{3.9}$$

one can use induction on the dimensions to obtain the lower bounds

$$b_{6k} \ge 3^k,$$
 $b_{6k+2} \ge 4 \cdot 3^{k-1},$
 $b_{6k+4} > 2 \cdot 3^k.$

Since 4 and 6 are even, the best lower bounds that we can get from (3.9) for odd dimensions n are $\flat_n \geq \flat_{n-1}$. On the other hand, the choir numbers are known to be finite (Wolpert, 1978; Suwa-Bier, 1984), although we are not aware of an explicit upper bound for their values in terms of the dimension n. As a closing remark, we conjecture that $\flat_4 = \flat_5 = 2$ and $\flat_6 = 3$.

Chapter 4

Beyond three terms: Neumann heat trace of convex polygons

In Chapter 2 we studied the spectral properties of integrable polygons, where the explicit expressions for the eigenvalues (2.1) allowed us to compute the heat trace explicitly and determine the precise form of the remainder in its short-time asymptotics. In this chapter, we turn to the more general case of convex polygons which are not necessarily integrable. Here we no longer have access to closed-form expressions for the eigenvalues, and new methods are required.

For Dirichlet boundary conditions, (van den Berg and Srisatkunarajah, 1988) established the short-time expansion (2.6), including an explicit estimate for the exponent c>0 in the remainder term. Their proof relied on probabilistic methods. Our aim here is to establish an analogous expansion for convex polygons with Neumann boundary conditions. Note, however, that the Neumann boundary condition is not well defined at the polygons' corners since they have no unique normal at those points. This difficulty can, however, be resolved by instead interpreting the Neumann problem in the weak sense. See Paper 4 for details.

The main difficulty with the Neumann case is that the Brownian mo-

tion approach in (van den Berg and Srisatkunarajah, 1988) cannot be applied. Indeed, van den Berg and Srisatkunarajah express the Dirichlet heat kernel on the polygon as the probability that a certain Brownian bridge never hits the boundary, and it is not at all clear how to express the Neumann heat kernel in a similar way. We therefore develop an entirely different method, based on *locality principles*, which will be introduced in the next section.

4.1 Locality principles

To estimate the Neumann heat trace on a polygonal domain Ω , we rely on the principle that the heat kernel $H_{\Omega}(t, x, x)$ can be approximated locally by those of model domains, depending on the position of $x \in \Omega$:

- Near a corner P_i with angle γ_i , $H_{\Omega}(t, x, x)$ is approximated by the heat kernel $H_{\gamma_i}(t, x, x)$ on an infinite sector with interior angle γ_i and Neumann boundary conditions.
- Near an edge but away from the corners, $H_{\Omega}(t, x, x)$ is approximated by the heat kernel $H_{\mathbb{R}^2_+}(t, x, x)$ on a Euclidean half-plane with Neumann boundary conditions.
- Away from the boundary, $H_{\Omega}(t, x, x)$ is approximated by the heat kernel $H_{\mathbb{R}^2}(t, x, x)$ on the Euclidean plane.

To formalize this idea, we use the notion of exact geometric matches, which was introduced in (Nursultanov et al., 2019). Let $\Omega_0, \Omega, S \subset \mathbb{R}^n$ be domains with $\Omega_0 \subset \Omega \cap S$. We say that S and Ω are exact geometric matches on Ω_0 if $\partial \Omega_0 \cap \partial \Omega = \partial \Omega_0 \cap \partial S$. This setting allows us to compare the heat kernels $H_{\Omega}(t, x, y)$ and $H_{S}(t, x, y)$ for points $x, y \in \Omega_0$ as $t \downarrow 0$.

4.1.1 General patchwork construction

Let $\Omega, \Omega_0, S \subset \mathbb{R}^n$ be domains such that S and Ω are exact geometric matches on Ω_0 , and assume that they are all equipped with the same boundary conditions. In (Nursultanov et al., 2019, Thm. 4), it is

shown that for Neumann and Robin boundary conditions one has

$$|H_{\Omega}(t,x,y) - H_{S}(t,x,y)| = \mathcal{O}(t^{\infty}), \ x,y \in \Omega_{0}, \ t \downarrow 0, \tag{4.1}$$

where the notation $\mathcal{O}(t^{\infty})$ indicates that the error decays faster than any power of t as $t \downarrow 0$. The corresponding statement for Dirichlet boundary conditions had been established earlier and is known as Kac's principle of feeling the boundary.

Note that (Nursultanov et al., 2019, Thm. 4) has certain assumptions on Ω and S, such as the (ϵ, h) -cone condition and that the second fundamental form of $\partial\Omega$ and ∂S are bounded below. However, such assumptions are satisfied in our setting where Ω is a convex polygon and S is either an infinite sector, the Euclidean half-plane, or the Euclidean plane, see (Nursultanov et al., 2019, Remark 1).

While (4.1) is sufficient for the purposes of (Nursultanov et al., 2019), it does not provide explicit control on the decay rate. For our application, however, such quantitative information is needed in order to obtain an explicit remainder estimate for the heat trace. We therefore outline the main ideas of the proof of (Nursultanov et al., 2019, Thm. 4), indicating how the argument can be adapted to make the decay rate explicit, and refer to Paper 4 for the full details. Throughout, by an ϵ -neighborhood of a subset $A \subset \Omega$ we mean

$$\{x \in \Omega : d(x, A) < \epsilon\},\$$

that is, neighborhoods are always taken relative to Ω rather than \mathbb{R}^2 .

Lemma 4.1.1. Let $\Omega, \Omega_0, S \subset \mathbb{R}^2$ be domains with Neumann boundary conditions such that S and Ω are exact geometric matches on Ω_0 . Assume further that $\Omega \subset S$. Finally, assume that the heat kernel $H_S(t, x, y)$ on S satisfies the bounds

$$|H_S(t,x,y)| \le \frac{C_1}{t^{m_1}} e^{-|x-y|^2/(4t)}, \ x,y \in S, \ t > 0,$$

$$|\nabla H_S(t,x,y)| \le \frac{C_2}{t^{m_2}} e^{-|x-y|^2/(4t)}, \ x,y \in S, \ t > 0,$$
(4.2)

Chapter 4. Beyond three terms: Neumann heat trace of convex polygons

for some $C_1, C_2, m_1, m_2 > 0$. Then, for any $\epsilon > 0$ such that an ϵ -neighborhood of Ω_0 and Ω are exact geometric matches on Ω_0 , and for any $T, \delta > 0$, there is a C > 0 such that

$$|H_{\Omega}(t, x, x) - H_{S}(t, x, x)| \le Ce^{-\epsilon^{2}/((4+\delta)t)}, \ x \in \Omega_{0}, \ 0 < t < T.$$
 (4.3)

The proof of Lemma 4.1.1 is based on a parametrix construction, which allows one to construct heat kernels whenever one has exact geometric matches on each part of the domain. The basic step is to glue together heat kernels on S using a certain smooth partition of unity on Ω . This produces an approximate heat kernel G, called patchwork heat kernel, which agrees exactly with H_S on Ω_0 .

We then define $E = (\partial_t + \Delta)G$ and note that it is supported away from Ω_0 . Moreover, it can be controlled using Gaussian bounds for H_S and its derivatives. These estimates show that E is exponentially small in t for $x, y \in \Omega$. By iteratively convolving E with itself, one constructs a Neumann series K, and shows that it inherits the same exponential decay. Finally, one writes

$$H_{\Omega} - G = -K * G$$

and estimates the right hand side to deduce the desired locality bound.

4.1.2 Partitioning of the polygon

Throughout this subsection, we assume that every domain has Neumann boundary conditions. To apply Lemma 4.1.1 and derive locality estimates, we partition the convex polygon Ω into regions that are locally modeled by simpler domains: the infinite sector S_{γ} , the Euclidean half-plane \mathbb{R}^2_+ , and the Euclidean plane \mathbb{R}^2_- . As usual, let $\gamma_1, \ldots, \gamma_n$ denote the interior angles of Ω . Following (van den Berg and Srisatkunarajah, 1988), we define the minimal interior angle

$$\gamma := \min_{i} \gamma_{i}, \tag{4.4}$$

and for each corner P_i , we define for r > 0

$$B_i(r) := \{ x \in \Omega : d(x, P_i) < r \}. \tag{4.5}$$

We also introduce

$$R := \frac{1}{2} \sup \left\{ r > 0 : B_i(r) \cap B_j(r) = \emptyset \ \forall i \neq j, \ \bigcup_{k=1}^n B_k(r) \subset \Omega \right\}.$$
 (4.6)

Then we define

$$C(R,\gamma) := \{ x \in \Omega : d(x,\partial\Omega) < R \sin(\gamma/2)/2, \ x \notin \bigcup_{i=1}^{n} B_i(R) \},$$

$$D(R,\gamma) := \{ x \in \Omega : x \notin \bigcup_{i=1}^{n} B_i(R), \ x \notin C(R,\gamma) \}.$$

The set $C(R, \gamma)$ contains points near the edges but away from the corners, and $D(R, \gamma)$ contains points in the interior away from the boundary. See Paper 4 for an illustration. Altogether, these form a partition of the polygon:

$$\Omega = \bigsqcup_{i=1}^{n} B_i(R) \sqcup C(R, \gamma) \sqcup D(R, \gamma).$$

Each of the regions is contained in a subdomain of Ω that is isometric to a subdomain of one of the model domains, allowing us to apply Lemma 4.1.1 in each case.

Lemma 4.1.2 (Locality principle at a corner). Let P_i be a corner of the convex polygon Ω with angle γ_i . For any $T, \delta > 0$, there is a C > 0 such that

$$|H_{\Omega}(t, x, x) - H_{\gamma_i}(t, x, x)| \le Ce^{-R^2/((4+\delta)t)}, \ x \in B_i(R),$$

 $0 < t < T.$ (4.7)

Proof idea. Since Ω is convex, it can be identified with a subdomain of the infinite sector S_{γ_i} . Gaussian bounds and gradient estimates for the heat kernel on convex domains, in particular S_{γ_i} , allow us to verify the assumptions of Lemma 4.1.1. Thus, for any ϵ such that Ω and $B_i(R + \epsilon)$ are exact geometric matches on $B_i(R)$, we have

$$|H_{\Omega}(t, x, x) - H_{\gamma_i}(t, x, x)| \le Ce^{-\epsilon^2/((4+\delta)t)}, \ x \in B_i(R), \ 0 < t < T,$$

for some C > 0. Choosing $\epsilon = R$ gives the desired bound.

Chapter 4. Beyond three terms: Neumann heat trace of convex polygons

Lemma 4.1.3 (Locality principle at an edge). Let Ω be a convex polygon. For any $T, \delta > 0$, there is a C > 0 such that

$$|H_{\Omega}(t, x, x) - H_{\mathbb{R}^{2}_{+}}(t, x, x)| \le Ce^{-R^{2}\sin^{2}(\gamma/2)/(4(4+\delta)t)},$$

$$x \in C(R, \gamma), \ 0 < t < T.$$
(4.8)

Proof idea. Near the midpoint of an edge, Ω is locally modeled by the half-plane \mathbb{R}^2_+ . The explicit reflection formula for the half-plane heat kernel,

$$H_{\mathbb{R}^{2}_{+}}(t,x,y) = \frac{e^{-|x-y|^{2}/(4t)} + e^{-|x-y^{*}|^{2}(4t)}}{4\pi t},$$
(4.9)

provides Gaussian and gradient bounds that again satisfy the hypotheses of Lemma 4.1.1. Then

$$|H_{\Omega}(t,x,x) - H_{\mathbb{R}^2}(t,x,x)| \le Ce^{-\epsilon^2/((4+\delta)t)}, \ x \in C(R,\gamma), \ 0 < t < T,$$

for any $\epsilon > 0$ such that an ϵ -neighborhood of $C(R, \gamma)$ and Ω are exact geometric matches on $C(R, \gamma)$. A geometric argument shows that we may choose $\epsilon = R \sin(\gamma/2)/2$, which gives the bound in the lemma. \square

Lemma 4.1.4 (Locality principle at the interior). Let Ω be a convex polygon. For any $T, \delta > 0$, there is a C > 0 such that

$$|H_{\Omega}(t, x, x) - H_{\mathbb{R}^2}(t, x, x)| \le Ce^{-R^2 \sin^2(\gamma/2)/(4(4+\delta)t)},$$

$$x \in D(R, \gamma), \ 0 < t < T.$$
(4.10)

Proof idea. We have

$$\begin{split} H_{\mathbb{R}^2}(t,x,y) &= \frac{1}{4\pi t} e^{-|x-y|^2/(4t)}, \\ \nabla H_{\mathbb{R}^2}(t,x,y) &= -\frac{x-y}{2t} H_{\mathbb{R}^2}(t,x,y). \end{split}$$

In particular, there are $C_1, C_2 > 0$ such that

$$|H_{\mathbb{R}^2}(t,x,y)| = \frac{C_1}{t} e^{-|x-y|^2/((4+\delta)t)}, \ x,y \in \Omega, \ t > 0,$$
$$|\nabla H_{\mathbb{R}^2}(t,x,y)| = \frac{C_2}{t^2} e^{-|x-y|^2/((4+\delta)t)}, \ x,y \in \Omega, \ t > 0.$$

Then, Lemma 4.1.1 gives that there is a C > 0 such that

$$|H_{\Omega}(t, x, x) - H_{\mathbb{R}^2}(t, x, x)| \le Ce^{-\epsilon^2/((4+\delta)t)}, \ x \in D(R, \gamma), \ 0 < t < T,$$

where $\epsilon > 0$ is such that an ϵ -neighborhood of $D(R, \gamma)$ has a positive distance to $\partial\Omega$. As in Lemma 4.1.3, we may choose $\epsilon = R\sin(\gamma/2)/2$, which gives the bound that we want.

4.2 Heat trace

Having established locality estimates for the Neumann heat kernel $H_{\Omega}(t, x, x)$ on different regions of the polygon, we now turn to the main result.

Theorem 4.2.1. Let $\Omega \subset \mathbb{R}^2$ be an n-sided convex polygon with angles $\gamma_1, \ldots, \gamma_n$. Let γ and R be as in (4.4) and (4.6), respectively, and let $h_{\Omega}(t)$ denote the Neumann heat trace. Then, for any $\delta > 0$, there is a C > 0 such that

$$\left| h_{\Omega}(t) - \frac{|\Omega|}{4\pi t} - \frac{|\partial\Omega|}{8\sqrt{\pi t}} - \sum_{i=1}^{n} \frac{\pi^2 - \gamma_i^2}{24\pi \gamma_i} \right| \le Ce^{-R^2 \sin^2(\gamma/2)/(4(4+\delta)t)}$$
 (4.11)

for all t > 0.

The key idea to proving Theorem 4.2.1 is to approximate $H_{\Omega}(t, x, x)$ by the corresponding model heat kernels on each subregion of Ω , using Lemmas 4.1.2-4.1.4, and then integrate the model heat kernels over each subregion. Applying these lemmas region by region yields

$$\left| h_{\Omega}(t) - \left(\sum_{i=1}^{n} \int_{B_{i}(R)} H_{\gamma_{i}}(t, x, x) dx + \int_{C(R, \gamma)} H_{\mathbb{R}^{2}_{+}}(t, x, x) dx + \int_{D(R, \gamma)} H_{\mathbb{R}^{2}}(t, x, x) dx \right) \right|$$

$$\leq C |\Omega| e^{-R^{2} \sin^{2}(\gamma/2)/(4(4+\delta)t)}, \quad 0 < t < T.$$
(4.12)

The next step is to compute the contributions from each model heat kernel explicitly. Following the approach of (van den Berg and Srisatkunarajah, 1988), we obtain in Paper 4

$$\int_{B_{i}(R)} H_{\gamma_{i}}(t, r, \theta, r, \theta) r dr d\theta$$

$$= \frac{\gamma_{i} R^{2}}{8\pi t} + \frac{R^{2}}{2\pi t} \int_{0}^{1} \frac{\sqrt{1 - y^{2}}}{e^{R^{2}y^{2}/t}} dy + \frac{\pi^{2} - \gamma_{i}^{2}}{24\pi \gamma_{i}} + A_{\gamma_{i}}(t),$$

$$\int_{C(R,\gamma)} H_{\mathbb{R}^{2}_{+}}(t, x, x) dx = \frac{|C(R, \gamma)|}{4\pi t} + \frac{|\partial \Omega|}{8\sqrt{\pi t}}$$

$$-\frac{|\partial \Omega|}{4\pi t} \int_{R\sin(\gamma/2)/2}^{\infty} e^{-y^{2}/t} dy - \frac{nR^{2}}{2\pi t} \int_{0}^{\sin(\gamma/2)/2} \frac{\sqrt{1 - y^{2}}}{e^{R^{2}y^{2}/t}} dy,$$

$$\int_{D(R,\gamma)} H_{\mathbb{R}^{2}}(t, x, x) dx = \frac{|D(R, \gamma)|}{4\pi t}.$$
(4.13)

Here, $A_{\gamma_i}(t)$ is given by (van den Berg and Srisatkunarajah, 1988, Eq. 2.2-2.4). In particular, we have by (van den Berg and Srisatkunarajah, 1988, Cor. 3)

$$|A_{\gamma_i}(t)| \le \left(\frac{\gamma_i}{8\pi} + \frac{3\pi^2}{64\gamma_i^2}\right) e^{-R^2 \sin^2(\gamma_i)/t}, \ t > 0.$$
 (4.14)

We insert (4.13) into (4.12) to obtain

$$\left| h_{\Omega}(t) - \sum_{i=1}^{n} \left[\frac{\gamma_{i} R^{2}}{8\pi t} + \frac{R^{2}}{2\pi t} \int_{0}^{1} \frac{\sqrt{1 - y^{2}}}{e^{R^{2}y^{2}/t}} dy + \frac{\pi^{2} - \gamma_{i}^{2}}{24\pi \gamma_{i}} + A_{\gamma_{i}}(t) \right] \right]
- \left[\frac{|C(R, \gamma)|}{4\pi t} + \frac{|\partial \Omega|}{8\sqrt{\pi t}} - \frac{|\partial \Omega|}{4\pi t} \int_{R\sin(\gamma/2)/2}^{\infty} e^{-y^{2}/t} dy \right]
- \frac{nR^{2}}{2\pi t} \int_{0}^{\sin(\gamma/2)/2} \frac{\sqrt{1 - y^{2}}}{e^{R^{2}y^{2}/t}} dy - \frac{|D(R, \gamma)|}{4\pi t} \right|
\leq C|\Omega| e^{-R^{2}\sin^{2}(\gamma/2)/(4(4+\delta)t)}, \quad 0 < t < T.$$

Since

$$\sum_{i=1}^{n} \frac{\gamma_i R^2}{8\pi t} + \frac{|C(R,\gamma)|}{4\pi t} + \frac{|D(R,\gamma)|}{4\pi t} = \frac{|\Omega|}{4\pi t},$$

this simplifies to

$$\begin{split} \left| h_{\Omega}(t) - \frac{|\Omega|}{4\pi t} - \frac{|\partial\Omega|}{8\sqrt{\pi t}} - \sum_{i=1}^{n} \frac{\pi^{2} - \gamma_{i}^{2}}{24\pi\gamma_{i}} - \frac{nR^{2}}{2\pi t} \int_{\sin(\gamma/2)/2}^{1} \frac{\sqrt{1 - y^{2}}}{e^{R^{2}y^{2}/t}} dy \right. \\ \left. - \sum_{i=1}^{n} A_{\gamma_{i}}(t) + \frac{|\partial\Omega|}{4\pi t} \int_{R\sin(\gamma/2)/2}^{\infty} e^{-y^{2}/t} dy \right| \\ \leq C|\Omega|e^{-R^{2}\sin^{2}(\gamma/2)/(4(4+\delta)t)}, \ 0 < t < T. \end{split}$$

We have the estimates

$$\int_{\sin(\gamma/2)/2}^{1} \frac{\sqrt{1-y^2}}{e^{R^2y^2/t}} dy \le e^{-R^2\sin^2(\gamma/2)/(4t)},$$

$$\int_{R\sin(\gamma/2)/2}^{\infty} e^{-y^2/t} dy \le \frac{t}{R\sin(\gamma/2)} e^{-R^2\sin^2(\gamma/2)/(4t)}.$$

Moreover, (4.14) gives

$$\sum_{i=1}^{n} |A_{\gamma_i}(t)| \le \left(\frac{n-2}{8} + \frac{3\pi^2 n}{64\gamma^2}\right) e^{-R^2 \sin^2(\gamma)/t}.$$

Hence, by the triangle inequality,

$$\begin{split} & \left| h_{\Omega}(t) - \frac{|\Omega|}{4\pi t} - \frac{|\partial\Omega|}{8\sqrt{\pi t}} - \sum_{i=1}^{n} \frac{\pi^{2} - \gamma_{i}^{2}}{24\pi\gamma_{i}} \right| \\ \leq & \left(\frac{nR^{2}}{2\pi t} + \frac{|\partial\Omega|}{4\pi R \sin(\gamma/2)} + \frac{n-2}{8} + \frac{3\pi^{2}n}{64\gamma^{2}} + C|\Omega| \right) e^{-R^{2} \sin^{2}(\gamma/2)/(4(4+\delta)t)}, \\ & 0 < t < T. \end{split}$$

In particular, there is a C > 0 such that (4.11) holds for 0 < t < T. This proves Theorem 4.2.1 for 0 < t < T. For $t \ge T$, recall from (1.7) that $h_{\Omega}(t)$ is bounded for $t \ge T$. Therefore,

$$\left| h_{\Omega}(t) - \frac{|\Omega|}{4\pi t} - \frac{|\partial\Omega|}{8\sqrt{\pi t}} - \sum_{i=1}^{n} \frac{\pi^2 - \gamma_i^2}{24\pi \gamma_i} \right|$$

is also bounded for $t \geq T$. It follows that there is a C > 0 such that (4.11) holds for $t \geq T$, from which Theorem 4.2.1 follows.

4.3 Compact polyhedral surfaces

In this section, we explain how we can use Theorem 4.2.1 together with the Dirichlet heat trace expansion (2.6) to obtain a corresponding short-time asymptotic expansion for the heat trace of compact polyhedral surfaces. As explained in (Hezari et al., 2017, p. 3766), from any polygon Ω we may form a compact Euclidean surface with conical singularities Σ by gluing together two copies of Ω along their boundaries. The resulting surface has vertices P_1, \ldots, P_n with angles twice the size of the interior angles of Ω , and the Friedrichs extension of the Laplacian on $C_0^{\infty}(\Sigma \setminus \{P_1, \ldots, P_n\})$ has spectrum equal to the union of the Dirichlet and Neumann spectra of Ω , counting multiplicity. In particular, the heat trace $h_{\Sigma}(t)$ of Σ satisfies

$$h_{\Sigma}(t) = h_{\Omega}^{D}(t) + h_{\Omega}^{N}(t),$$

where $h_{\Omega}^{D}(t)$ and $h_{\Omega}^{N}(t)$ are the Dirichlet and Neumann heat traces of Ω , respectively. Combining this with (2.6), Theorem 4.2.1, and the observation

$$\left(\frac{|\Omega|}{4\pi t} - \frac{|\partial\Omega|}{8\sqrt{\pi t}} + \sum_{i=1}^{n} \frac{\pi^2 - \gamma_i^2}{24\pi \gamma_i}\right) + \left(\frac{|\Omega|}{4\pi t} + \frac{|\partial\Omega|}{8\sqrt{\pi t}} + \sum_{i=1}^{n} \frac{\pi^2 - \gamma_i^2}{24\pi \gamma_i}\right) \\
= \frac{|\Omega|}{2\pi t} + \sum_{i=1}^{n} \frac{\pi^2 - \gamma_i^2}{12\pi \gamma_i},$$

we obtain the following result.

Theorem 4.3.1. Let $\Omega \subset \mathbb{R}^2$ be an n-sided convex polygon with vertices P_1, \ldots, P_n of interior angles $\gamma_1, \ldots, \gamma_n$. Let γ and R be as in (4.4) and (4.6), respectively. Let Σ be the corresponding compact polyhedral surface, and let Δ be the Friedrichs extension of the Laplacian on $C_0^{\infty}(\Sigma \setminus \{P_1, \ldots, P_n\})$. Then, for any $\delta > 0$, there is a C > 0 such that the heat trace $h_{\Sigma}(t)$ of Σ satisfies

$$\left| h_{\Sigma}(t) - \frac{|\Omega|}{2\pi t} - \sum_{i=1}^{n} \frac{\pi^2 - \gamma_i^2}{12\pi \gamma_i} \right| \le Ce^{-R^2 \sin^2(\gamma/2)/(4(4+\delta)t)}, \ t > 0.$$

Equivalently, if we denote the conical angles of Σ by β_1, \ldots, β_n , then

$$\left| h_{\Sigma}(t) - \frac{|\Sigma|}{4\pi t} - \sum_{i=1}^{n} \frac{4\pi^2 - \beta_i^2}{24\pi \beta_i} \right| \le Ce^{-R^2 \sin^2(\gamma/2)/(4(4+\delta)t)}, \ t > 0.$$

Chapter 5

Conclusions and future work

In this final chapter, we summarize the main contributions of the thesis and discuss possible directions for future research. The work has primarily focused on two fundamental classes of domains in spectral geometry, polygons and flat tori. The goal of this concluding discussion is to place these results in a broader context and to highlight natural questions that emerge from them.

5.1 Integrable polytopes and convergence of polygons

In Chapter 2, we used the explicit eigenvalue expressions (2.1) to compute several spectral invariants for the integrable polygons. A natural next step is to try to extend this analysis to three dimensions. The first step would then be to classify the 3-dimensional integrable polytopes. Intuitively, an n-dimensional polytope is a bounded domain in \mathbb{R}^n whose boundary is piecewise smooth and consists of (n-1)-dimensional flat faces. See (Rowlett et al., 2021, Def. 1) for a precise definition.

In two dimensions, a polygon is integrable if and only if it strictly tessellates the plane (McCartin, 2008) (Rowlett et al., 2021). This moti-

vates the following definition in higher dimensions: an n-dimensional polytope is called *integrable* if it strictly tessellates \mathbb{R}^n . Once the 3dimensional integrable polytopes have been identified, their spectral invariants can be obtained in much the same way as for polygons. In particular, by (Bérard, 1980), it is possible to explicitly compute the eigenvalues and eigenfunctions of the Laplacian on these domains with Dirichlet boundary conditions. This makes it possible to compute the corresponding spectral zeta function and heat trace by the same methods used for the 2-dimensional case. A particularly interesting question is whether the short-time asymptotics of the heat trace of 3dimensional integrable polytopes have an exponential decay analogous to that of the polygonal case. For integrable polygons, we found that the remainder term in the heat trace expansion decays exponentially with an exponent arbitrarily close $L^2/4$, where L denotes the length of the shortest closed geodesic (see Theorem 2.2.2). It would be interesting to determine whether this relationship also holds in three and higher dimensions.

In Chapter 2, we also examined the behavior of the heat trace coefficients when smoothly bounded convex domains converge in the Hausdorff sense to a convex polygon, and vice versa. We observed that when smooth domains converge to a polygon, the third heat trace coefficient does not converge, reflecting the geometric singularities introduced by the corners. In particular, the third heat trace coefficient equals 1/6 for smooth convex domains, whereas for polygons it is always greater than 1/6 (see Theorem 2.3.2). It would be interesting to investigate whether the remaining heat trace coefficients converge to those of the limiting polygon. Conversely, when convex polygons converge to a smoothly bounded domain, we found that the third heat trace coefficient does converge (see Theorem 2.3.3). In this case, it would be natural to explore whether the other coefficients, or even the entire heat trace, converge to those of the smooth domain. We note that the convexity assumption plays an essential role: if non-convex polygons converge in the Hausdorff sense to a smoothly bounded domain, the perimeters may diverge, and consequently the second heat trace coefficient need not converge.

5.2 Isospectral flat tori and choir numbers

In Chapter 3, we presented the first known example of a 6-dimensional triplet of mutually isospectral and non-isometric flat tori, thereby proving that the sixth choir number satisfies $b_6 \geq 3$. Recall that, for each dimension n, the nth choir number b_n is defined as the maximal k such that there exist k mutually isospectral and non-isometric n-dimensional flat tori. A natural continuation of this research is to search for additional isospectral non-isometric tuples of flat tori in various dimensions. In our investigation, we explored dimensions 4 through 9 quite extensively. In dimensions 4 and 5, we found many pairs (many likely new), but no triplets. In dimension 8 we found a triplet, and in dimension 9 we found four quadruplets, which were also likely new. However, among these results, only the 6-dimensional triplet provided new information regarding the choir numbers, which is why we chose to present it in detail. Indeed, since $b_4 \geq 2$ by Schiemann (Schiemann, 1990) and the choir numbers are supermultiplicative, it follows that $b_8 \geq 4$ and $b_9 \geq 4$, consistent with our findings. Searching in higher dimensions quickly becomes computationally expensive, which is why our explorations were limited to dimensions up to 9. Nevertheless, an obvious direction for future research is to develop more efficient algorithms or theoretical criteria for constructing or excluding large isospectral non-isometric tuples in higher dimensions, potentially revealing new information about the behavior of choir numbers beyond dimension 9.

Schiemann's method for finding the 4-dimensional pair of isospectral non-isometric flat tori was quite different from our approach. Instead of searching directly in the space of lattices or linear codes, he considered 4-dimensional integer quadratic forms. As explained in Chapter 3, two quadratic forms with the same representation numbers that are not integrally equivalent correspond precisely to two isospectral non-isometric flat tori. It is straightforward to see that such quadratic

forms must have the same determinant. Using this observation, Schiemann implemented a computer program that, for each positive integer k, searched through all 4-dimensional quadratic forms of determinant k to identify any pairs with identical representation numbers that are non-integrally equivalent. He carried out this search for all determinants up to 3000, and in doing so, found exactly one pair, which has determinant 1729 (Schiemann, 1990). Schiemann did not provide further details on how he enumerated all integer quadratic forms with a given determinant, so it remains unclear how to fully implement this method in practice. Nevertheless, it seems likely that this approach, like ours, would become computationally infeasible in dimensions higher than 9.

Instead of focusing solely on finding larger tuples to obtain better lower bounds for the choir numbers, one can also attempt to obtain upper bounds. For example, Schiemann used a computer-assisted method to prove that $b_3 = 1$ (Schiemann, 1994, 1997). His approach involves embedding the 3-dimensional quadratic forms into \mathbb{R}^6 and performing coverings and refinements of certain polyhedral cones in a highly technical procedure. See (Nilsson et al., 2023, Ch. 5) for a detailed explanation of the algorithm. One natural approach to obtaining upper bounds in higher dimensions would be to try to extend Schiemann's algorithm. However, this faces several challenges. First, one requires a notion of a reduced form for quadratic forms that ensures each equivalence class of integrally equivalent forms contains exactly one representative. Schiemann constructs such a reduced form (referred to as Schiemann reduced in (Nilsson et al., 2023, Ch. 5)), but it is unclear how to generalize this construction to higher dimensions. Second, the computational complexity becomes problematic. Even in three dimensions, running Schiemann's algorithm takes several hours, and extending it to higher dimensions or higher tuples (for instance, attempting to show that no 4-dimensional triplets exist, instead of showing that there are no 3-dimensional pairs) may quickly become infeasible. A direction for future research is therefore to seek a simpler, possibly computer-free, proof that $b_3 = 1$, and investigate whether

such a proof could be adapted to obtain upper bounds for the choir numbers in higher dimensions.

5.3 Heat trace expansion for Neumann polygons

In Chapter 4, we obtained an explicit estimate for the exponential decay in the remainder term of the Neumann heat trace expansion for convex polygons (see Theorem 4.2.1). To the best of our knowledge, this is the first time such an estimate has been obtained. However, it is not believed to be optimal. In Chapter 2, the precise exponential decay rate is determined for the integrable polygons. The result (see Theorem 2.2.2) shows that for integrable polygons with either Dirichlet or Neumann boundary conditions, the exponential decay rate in the remainder term can be made arbitrarily close to $L^2/4$, where L denotes the length of the shortest closed geodesic of the polygon. While $L^2/4$ provides a much sharper rate than that obtained in Theorem 4.2.1, the locality principles developed in Chapter 4 do not appear sufficient to recover the optimal exponent in the general case. Similarly, the probabilistic techniques used in (van den Berg and Srisatkunarajah, 1988) for Dirichlet boundary conditions do not seem capable of reaching the sharp exponent either. Achieving the sharp rate of decay likely requires a more global spectral analysis, capable of capturing the contribution of closed geodesics, as well as refined asymptotics for the eigenvalues. Developing such methods remains an open problem and would represent a significant advance in the understanding of spectral invariants of general polygonal domains.

In Theorem 4.2.1, the remainder in the asymptotic expansion (4.11) is controlled by an exponentially decaying term of the form $Ce^{-\alpha/t}$. While we have provided an explicit estimate for the exponent α , the coefficient C remains unspecified. It is therefore natural to ask whether it is possible to obtain an upper bound for C. One approach is to track the constants appearing in the proofs of Lemmas 4.1.1-4.1.4 and

Theorem 4.2.1. However, while many constants in the proof of Theorem 4.2.1 are estimated, carrying this out in Lemmas 4.1.1-4.1.4 leads to several technical challenges. First, the lemmas rely on heat kernel bounds on various model domains. To obtain an explicit constant C, one would need to control the constants appearing in these model heat kernel estimates. While Gaussian upper bounds are well known for many of these cases, obtaining precise constants, especially in sectors with Neumann boundary conditions, appears to be non-trivial. Second, the proof of Lemma 4.1.1 involves a smooth partition of unity and associated smooth cut-off functions, as detailed in Paper 4. Estimating the coefficient C in front of the exponential decay requires controlling the derivatives and supports of the cut-off functions, which in turn depend on the geometry of the domain in subtle ways. Finally, in the proof of Theorem 4.2.1, an explicit upper bound for the coefficient C would require an explicit upper bound for the heat trace $h_{\Omega}(t), t \geq T$. While we have (1.7) by Weyl's law, making this bound explicit is considerably more difficult. In particular, it would require detailed information about the Neumann spectrum of the polygon, which is generally not available in closed form. For Dirichlet boundary conditions, one could inscribe the polygon by a rectangle and apply the domain monotonicity property of the Dirichlet eigenvalues (Borthwick, 2020, Thm. 6.20). However, such a domain monotonicity property does not hold for Neumann boundary conditions. As a result, while Theorem 4.2.1 extends to all t > 0 by appealing to boundedness for large t, obtaining an explicit bound on C remains out of reach.

Another interesting and natural question is whether Lemmas 4.1.1-4.1.4 and Theorem 4.2.1 can be extended to non-convex polygons. However, such an extension encounters two main issues. The first issue is geometric. In the convex case, each corner neighborhood of Ω is isometric to a subdomain of the corresponding infinite sector S_{γ_i} . This is used several times in the proofs of Lemmas 4.1.1-4.1.2 (see Paper 4). For non-convex polygons, however, such identifications are not always compatible across corners. If a corner P_i with $\gamma_i > \pi$ is adjacent to a corner P_j with $\gamma_j < \pi$, then Ω cannot be placed inside S_{γ_j} so that

 P_j coincides with the vertex of the sector, because the neighboring part of P_i necessarily extends outside the sector. The second issue is analytic and concerns the heat kernel bounds on infinite sectors. In the convex case, where each interior angle γ_i satisfies $\gamma_i < \pi$, the sector S_{γ_i} is itself convex, and the heat kernel $H_{\gamma_i}(t, x, y)$ satisfies Gaussian upper bounds, see e.g. (Frank and Larson, 2024, Lemma 2.9). When Ω is non-convex, however, we have $\gamma_i > \pi$ for some i. Then S_{γ_i} is non-convex, and to the best of our knowledge, it is no longer clear if such bounds hold for the heat kernel and its gradient. Due to these complications, the extension of Lemmas 4.1.1-4.1.4 and Theorem 4.2.1 to non-convex polygons remains an open problem. It would likely require new insights into the behavior of the heat kernel on non-convex sectors and a more flexible comparison principle that does not rely on domain inclusion.

Finally, it is natural to ask whether the methods developed in Chapter 4 can be extended to treat the case of Robin boundary conditions. In (Nursultanov et al., 2019, Sec. 2.4), locality principles of the form (4.1) are established. By following their argument, it is straightforward to verify that locality principles analogous to Lemmas 4.1.1-4.1.4 continue to hold for convex polygons with Robin boundary conditions, once they are known in the Neumann case. However, the exponential decay is weaker in the Robin case than in the Neumann case. The main difficulty in extending Theorem 4.2.1 to Robin boundary conditions lies in computing the contribution of the model heat kernels to the heat trace. For the infinite sector S_{γ} , the Green's function for Robin boundary conditions can be obtained using the techniques in (Nursultanov et al., 2024, Appendix A), but computing its contribution to the heat trace appears to be a non-trivial task. Moreover, the heat kernel on the Euclidean half-plane with Robin boundary conditions contains an additional term compared to the Neumann heat kernel. This extra term contributes a non-exponentially decaying series to the heat trace. Specifically, it gives rise to an $\mathcal{O}(1)$ term, followed by terms of order \sqrt{t} , t, and so on; see (Nursultanov et al., 2019, Sec. 3.2). As a result, the heat trace expansion for convex polygons with Robin boundary conditions appears to contain infinitely many non-zero terms, in contrast to the three-term structure followed by exponential decay that holds in the Dirichlet and Neumann cases. To summarize, while the locality principles can be adapted to the Robin case, computing the full asymptotic expansion of the heat trace appears to be significantly more difficult.

Bibliography

- Aldana, C. L. and Rowlett, J. (2018). A polyakov formula for sectors. The Journal of Geometric Analysis, 28(2):1773–1839.
- Aurell, E. and Salomonson, P. (1994). On functional determinants of laplacians in polygons and simplicial complexes. *Communications in Mathematical Physics*, 165(2):233–259.
- Bérard, P. H. (1980). Spectres et groupes cristallographiques i: Domaines euclidiens. *Inventiones mathematicae*, 58(2):179–199.
- Borthwick, D. (2020). Spectral theory. Springer.
- Cerviño, J. M. and Hein, G. (2011). The conway–sloane tetralattice pairs are non-isometric. *Advances in Mathematics*, 228(1):153–166.
- Chowla, S. and Selberg, A. (1949). On epstein's zeta function (i). *Proceedings of the National Academy of Sciences*, 35(7):371–374.
- Conway, J. H. and Fung, F. Y. (1997). The sensual (quadratic) form. Number 26. Cambridge University Press.
- Conway, J. H. and Sloane, N. J. (1992). Four-dimensional lattices with the same theta series. *International Mathematics Research Notices*, 1992(4):93–96.
- Durso, C. (1988). On the inverse spectral problem for polygonal domains. PhD thesis, Massachusetts Institute of Technology.
- Earnest, A. and Nipp, G. (1991). On the theta series of positive

56 Bibliography

quaternary quadratic forms. CR Math. Rep. Acad. Sci. Canada, 13(1):33–38.

- Frank, R. L. and Larson, S. (2024). Riesz means asymptotics for dirichlet and neumann laplacians on lipschitz domains. arXiv preprint arXiv:2407.11808.
- Fursaev, D. (1994). The heat-kernel expansion on a cone and quantum fields near cosmic strings. *Classical and Quantum Gravity*, 11(6):1431.
- Gordon, C., Webb, D., and Wolpert, S. (1992). Isospectral plane domains and surfaces via riemannian orbifolds. *Inventiones mathematicae*, 110(1):1–22.
- Gutkin, E. (1986). Billiards in polygons. *Physica D: Nonlinear Phenomena*, 19(3):311–333.
- Hezari, H., Lu, Z., and Rowlett, J. (2017). The neumann isospectral problem for trapezoids. In *Annales Henri Poincaré*, volume 18, pages 3759–3792. Springer.
- Hezari, H., Lu, Z., and Rowlett, J. (2021). The dirichlet isospectral problem for trapezoids. *Journal of Mathematical Physics*, 62(5).
- Kac, M. (1966). Can one hear the shape of a drum? The american mathematical monthly, 73(4P2):1–23.
- Kitaoka, Y. (1977). Positive definite quadratic forms with the same representation numbers. *Archiv der Mathematik*, 28(1):495–497.
- Kneser, M. (1967). Lineare relationen zwischen darstellungsanzahlen quadratischer formen. *Mathematische Annalen*, 168(1):31–39.
- Kokotov, A. (2009). Compact polyhedral surfaces of an arbitrary genus and determinants of laplacians. arXiv preprint arXiv:0906.0717.
- Levitin, M., Mangoubi, D., and Polterovich, I. (2023). *Topics in spectral geometry*, volume 237. American Mathematical Society.

 $\S Bibliography$ 57

Mårdby, G. (2023). The mathematics of hearing the shape of a drum and filling kac's holes. Master's thesis.

- Mårdby, G. and Rowlett, J. (2024). 112 years of listening to riemannian manifolds. arXiv preprint arXiv:2406.18369.
- McCartin, B. J. (2008). On polygonal domains with trigonometric eigenfunctions of the laplacian under dirichlet or neumann boundary conditions. *Applied Mathematical Sciences*, 2(58):2891–2901.
- McKean Jr, H. P. and Singer, I. M. (1967). Curvature and the eigenvalues of the laplacian. *Journal of Differential Geometry*, 1(1-2):43–69.
- Milnor, J. (1964). Eigenvalues of the laplace operator on certain manifolds. *Proceedings of the National Academy of Sciences*, 51(4):542–542.
- Nilsson, E., Rowlett, J., and Rydell, F. (2023). The isospectral problem for flat tori from three perspectives. *Bulletin of the American Mathematical Society*, 60(1):39–83.
- Nursultanov, M., Rowlett, J., and Sher, D. (2019). How to hear the corners of a drum. In 2017 MATRIX Annals, pages 243–278. Springer.
- Nursultanov, M., Rowlett, J., and Sher, D. (2024). The heat kernel on curvilinear polygonal domains in surfaces. *Annales mathématiques du Québec*, pages 1–61.
- Pleijel, Å. (1954). A study of certain green's functions with applications in the theory of vibrating membranes. Arkiv för matematik, 2(6):553–569.
- Ray, D. B. and Singer, I. M. (1971). R-torsion and the laplacian on riemannian manifolds. *Advances in Mathematics*, 7(2):145–210.
- Rowlett, J., Blom, M., Nordell, H., Thim, O., and Vahnberg, J. (2021). Crystallographic groups, strictly tessellating polytopes, and analytic eigenfunctions. *The American Mathematical Monthly*, 128(5):387–406.

58 Bibliography

Schiemann, A. (1990). Ein beispiel positiv definiter quadratischer formen der dimension 4 mit gleichen darstellungszahlen. Archiv der Mathematik, 54(4):372–375.

- Schiemann, A. (1994). Ternäre positiv definite quadratische formen mit gleichen darstellungszahlen. (No Title).
- Schiemann, A. (1997). Ternary positive definite quadratic forms are determined by their theta series. *Mathematische Annalen*, 308(3):507–517.
- Shiota, K. (1991). On theta series and the splitting of $S_2(\Gamma_0(q))$. Journal of Mathematics of Kyoto University, 31(4):909–930.
- Suwa-Bier, Y. (1984). Positiv definite quadratische Formen mit gleichen Darstellungsanzahlen. na.
- van den Berg, M. and Srisatkunarajah, S. (1988). Heat equation for a region in \mathbb{R}^2 with a polygonal boundary. *Journal of the London Mathematical Society*, 2(1):119–127.
- Watanabe, K. (2000). Plane domains which are spectrally determined. Annals of Global Analysis and Geometry, 18(5):447–475.
- Weyl, H. (1912). Das asymptotische verteilungsgesetz der eigenwerte linearer partieller differentialgleichungen (mit einer anwendung auf die theorie der hohlraumstrahlung). *Mathematische Annalen*, 71(4):441–479.
- Wolpert, S. (1978). The eigenvalue spectrum as moduli for flat tori. Transactions of the American Mathematical Society, 244:313–321.